Title
Uncharted Waters: Super-Concentrated Electrolytes

Journal
Joule, 4(1)

ISSN
2542-4351

Authors
Borodin, Oleg
Self, Julian
Persson, Kristin A
et al.

Publication Date
2020

DOI
10.1016/j.joule.2019.12.007

Peer reviewed

Uncharted Waters: Super-concentrated Electrolytes

Oleg Borodin [1, 2*], Julian Self [3, 4], Kristin Persson [3, 4*], Chunsheng Wang [5*], Kang Xu [1, 2*]

1. Joint Center for Energy Storage Research, U.S. Army Research Laboratory, Adelphi, MD 20783, USA
2. Electrochemistry Branch, Sensors and Electron Devices Directorate, U.S. Army Research Laboratory, Adelphi, MD 20783, USA
3. Energy Technologies Area, Lawrence Berkeley National Laboratory, Berkeley, CA 94720, USA
4. Department of Materials Science and Engineering, University of California, Berkeley, CA 94720, USA
5. Department of Chemical and Biomolecular Engineering, University of Maryland College Park, MD 20742, USA

Abstract

As a legacy left behind by classical analytical electrochemistry in pursuit of ideal electrodics, and classical physical electrochemistry in pursuit of the most conductive ionics, the study of non-aqueous electrolytes has been historically confined within a narrow concentration regime around 1 molarity (M). This confinement was breached in recent years when unusual properties were found to arise from the excessive salt presence, which often bring benefits to mechanical, thermal, transport, interfacial and interphasial properties that are of significant interest to electrochemical energy storage community. This perspective article provides an overview on this newly discovered and under-explored realm, with emphasis placed on their applications in rechargeable batteries.

1. History of the Art: Legacy and Deviation

Since the dawn of electrochemistry, high salt concentration in electrolytes has never been favored. While the analytic school of electrochemistry focused on producing accurate mathematic descriptions of electrodic behaviors in the ideal state free of interionic interferences,[1-3] a requirement that can only be met when the ions under investigation be kept at infinitesimal, the physical school of electrochemistry pursued the practical application of electrochemical devices, where the optimum ionic transport is of primary importance.[4-6] The "*1 molarity (M) legacy*" of non-aqueous electrolytes originated from such pursuits, because the maxima of ionic conductivities almost always occur at the salt concentration of 1.0 M for all systems. These maxima are the results of compromise between two major contributors to transport properties: (1) ionic carrier number (n) proportional to the salt dissolution and dissociation and (2) ionic mobility (μ) associated with the matrix viscosity (η) of electrolyte (Figure 1). Such relation holds true for systems where the movement of an ion is highly coupled with its surroundings (i.e., solvent

molecules) via the solvation sheath. The most extreme case is perhaps the solid-polymer-electrolytes, which can be viewed as macromolecular version of non-aqueous electrolytes.[7] In those highly coupled electrolyte systems, the ionic transport cannot happen without the cooperative movement of polymeric segments that solvate the ions. It was the belief that the above ion-solvent coupling would keep intensifying with increasing salt concentration that had discouraged interest in exploring the super-concentration realms.

The beneficial aspects of the saturated electrolytes were noticed as far back as 1985 by McKinnon and Dahn, who reported that a saturated PC solution of $LiAsF_6$ demonstrated unusual electrochemical intercalation behavior toward a layered host that could not be possible in *1M* electrolyte.[8] However, the earliest serious attempt to breach the concentration confinement ironically happened with polymer electrolytes. In order to free Li^+-movement from the traps formed by its polymeric solvation cages, Angell *et al*. ventured into the "uncharted waters" of super-concentration (Figure 2).[9] The "*polymer-in-salt*" concept proposed involved polymers being added as minority to the bulk molten salt or a salt mixture in order to lower the melting point, in the hope that the polymer as mechanic skeleton would impart its rubbery characteristic while the salt maintains most of the ionic movement without negative effects from polymeric traps. Although "*polymer-in-salt*" concept eventually encountered the practical difficulty of finding room-temperature molten salts with an electrochemical stability window wide enough to support meaningful battery chemistries, it did reveal that unexpected benefits might arise beyond and away from the narrow confinement of diluted salt concentration. Similar concept now is being actively explored in the development of the polymer-electrolyte-in-ceramic hybrid electrolytes with the interfacial region being the key to optimizing the overall ionic transport.[10; 11]

A decade later, unusual interphasial properties were noticed with a similar venture in liquid non-aqueous electrolyte. According to Jeong et al.,[12] the well-known exfoliation of graphite by propylene carbonate (PC) would not happen when some lithium salts are used at a higher-than-usual concentration. However, the general enthusiasm in super-concentrated electrolytes was not initiated until another decade later, when Watanabe and co-workers described a series of unusual properties from the glyme-based super-concentrated electrolytes.[13-17]

2. State of the Art: Super-concentration and Its Derivatives

Considered a transition regime between the conventional "1 M" electrolytes and neat ionic liquids or molten salts, the so-called "*super-concentrated electrolytes*" do not have a clear and quantitative definition. Depending on the nature of the solvents and the corresponding capability of dissolving salts, the salt concentration involved ranges from 3~5 M in non-aqueous media up to 4~10 M in aqueous media. At these high salt concentrations, significant ion–pairing and aggregation occurs, while limited solvent molecules therein are largely bound to cations, leading to entirely new structures at both molecular and long-range scales that affects a host of properties covering transport, thermal, mechanical, electrochemical, interfacial and interphasial.

Instead of defining a finite concentration limit, we can tentatively classify all electrolytes into three distinct regimes by looking at how ion solvation sheath is structured, as shown in Figure 3:

(1) "*Salt-in-solvent*" electrolytes, where the population of solvent molecules is higher than needed to complete the primary solvation sheath for the cations;

(2) "*Salt-solvate*" electrolytes, where the population of solvent molecules is just sufficient to complete the primary solvation sheath for the cations, so that stoichiometric solvates often form for the largely dissociating salts;

(3) "*Solvent-in-salt*" electrolytes, where the primary solvation sheath for the cation cannot be completed due to insufficient solvent population.

While the conventional electrolytes at ~1.0 M belongs to "salt-in-solvent" category, super-concentrated electrolytes are covered by the latter two categories, with the "salt-solvates" also often referred to as "quasi-ionic liquids" or "solvated ionic liquids" in order to highlight their similarity to room-temperature ionic liquids (RTILs) due to low fraction of "free" solvent. The primary limiting condition on whether a super-concentrated electrolyte exists or not is apparently the solubility of a salt in a given solvent that is related to the melting point of solvates, disorder and crystallization kinetics that can give rise the crystallinity and gaps at high salt concentration.[18; 19] While the high donicity of ether molecules makes them the popular choices, the weakly associated anions such as bis(trifluoromethanesulfonyl)imide (TFSI) can ensure maximum ion dissociation. Using ether molecules of varying length such as triglyme (G3) or tetraglyme (G4), Watanabe and coworkers demonstrated that the tight binding of all glyme molecules by high ionic populations (Figure 4a) induced a series of dramatic properties that are otherwise impossible at dilute salt concentrations, [13-17; 20] the most representative of which include the thermal stability up to 200ºC (Figure 4b) and altered electrochemical behaviors on both cathode (see Figure 4c for performance on Pt), improved stability against the $LiCoO_2$ cathode compared to 1 M analogs when charged to 4.2 V,[14] and graphitic anode (Figure 4d, supporting reversible Li^+-intercalation chemistry without the co-intercalation behavior typically associated with ethers). They attributed the emergence of these unusual properties to the solvation of high population of Li^+ by limited population of solvent (glyme) molecules, resulting in elimination of "free" solvent.

Among the numerous candidates as potential solvents and salts to make an electrolyte super-concentrated, two classes of compounds have been receiving special favors due to their unique properties: *ethereal solvents* for their strong dissolution and chelating capabilities toward cations and *imide-based salts* (LiTFSI, or its homologs such as lithium bis(pentafluoroethanesulfonyl)imide, LiBETI, or lithium bis(fluorosulfonyl)imide, LiFSI) for their extra-ordinary tendency to dissolve and dissociate in almost all polar solvents. Most of the successful super-concentrated electrolytes rely on at least one of these components, with the successful examples include the "*solvent-in-salt*" electrolytes of Suo et al based on LiTFSI dissolved in 1,2-dimethoxy ethane (DME) and 1,3-dioxolane (DOL) at concentrations up to 7 M,[21] the "*super-concentrated*" electrolytes of Yamada *et al.*[22] based on either LiTFSI dissolved in acetonitrile up to 4 M or LiFSI dissolved in dimethyl carbonate up to 10 m,[23] or the "*self-*

extinguishing electrolytes" of Shiga *et al*[24] based on NaFSI or LiFSI dissolved in phosphate esters or amides up to 3 M.

Perhaps the most extreme scenario of super-concentrated electrolytes are the so-called "*water-in-salt*" electrolyte (WiSE) by Suo et al. based on LiTFSI dissolved in water at concentrations up to 21 m (or ≈5 M)[25] and the many variations including sodium and zinc electrolyte,[26-31] which have brought unprecedented electrochemical stabilities to aqueous electrolytes and enabled revolutionary aqueous battery chemistries that were otherwise impossible (Figure 5).[32-34]

To minimize the high cost disadvantage induced by high salt concentration, there have been numerous efforts towards reducing the salt usage without compromising the advantages brought by super-concentration, such as preferred ion transport, non-flammability and interfacial/interphasial stabilities. One innovative approach is the so-called "*localized high concentration electrolytes*", where a Li^+ non-coordinating co-solvent (usually a polyfluorinated ether) was used to dilute the parental electrolyte, so that the overall salt concentration in electrolyte would rest in the more conventional range near 1.0 M rather than super-concentration (Figure 6).[35-39] The essence of such strategy is to separate the bulk and interfacial responsibilities of an electrolyte and assign these roles to varying phases that are microscopically separated. In all the electrolyte compositions reported, such role-separation leverages the poor solvation of Li^+ or Na^+ by various fluorinated molecules. Thus, while the immediate local environment of cations (Li^+, or Na^+) still maintains the solvation structure of super-concentrated electrolytes, which is often responsible for the interphasial chemistries at electrode surfaces, the bulk properties (ion transport, viscosity or wettability toward the electrodes and separators) were mainly defined by the average composition of the bulk electrolyte that still bear the nature of diluted regime. The simultaneous stabilization of the lithium metal and high capacity/voltage cathodes might have benefited from the highly fluorinated CEI formed by the partially fluorinated non-solvent and the defluorination of both LiFSI and $LiPF_6$,[40; 41] while most of the "oxidatively weak" but highly Li^+-solvating solvents were kept away due to the coulombic repulsion at the cathode surface.[42] Because the strong salt aggregation is preserved locally in the electrolyte as a non-coordinated diluent is added, the preferential salt reduction that requires such aggregation is also preserved in the diluted regime.[29; 42] From this prospective, the electrolyte based on mixture of coordinating and fluorinated/non-coordinating co-solvent also fits the framework of the "*localized high concentration electrolytes*" if the fraction of the non-coordinated co-solvent is sufficiently high.[29]

In several cases, exotic solvent systems traditionally thought impossible have also been used, such as ether or alkylphosphate esters, achieving both bulk and interfacial benefits, in addition to the cost reduction because of the lower apparent salt concentration. To some degree this design principle is a logical extension of the original design of the lithium ion battery electrolytes comprised from the mixtures of ethylene carbonate (EC) and dimethyl carbonate (DMC), where EC role was to stabilize graphite anode and dissociate salt, while DMC or other cycle carbonate reduced electrolyte viscosity and lowered its melting point.[43] As the mechanism

and dynamics of this class of electrolytes become better understood, there should be plenty of new solvent-salt combinations to emerge.

3. Solvation and Liquid Structure

Electrolyte is responsible for providing electric current between cathode (positive) and anode (negative), and such current that be solely carried by moving ions. With the rare exceptions of salts in molten (ionic liquid) or decoupled ceramic/glassy states, majority of these mobile ions come from the dissociation of salts by polar solvent molecules.[43] The resultant solvated ions constitute the actual ionic species that are mobile in electrolytes. Apparently how these ions interact with solvent molecules and among themselves define a series of parameters of the resultant electrolytes, ranging from mechanical (compressibility, viscosity), thermal (heat conductivity and capacity), to chemical (solubility, activity, reactivity), transport and electrochemical (interfacial and interphasial). Most of these properties are key in dictating the performance of any electrochemical devices.

The classical Debye-Hückel model assumes complete dissociation of salt while ignoring direct solvent-salt interactions beyond providing mean-field like screening through permittivity, while modern ionics recognizes the vital importance of polar solvent molecules in stabilizing the ions in dissociated form.[5] Bernal and Fowler were the pioneers who quantified how the introduction of an ion into bulk solvent induces the neighboring solvent molecules to reorient their dipoles around this ion, thus breaking the structure of the bulk solvent.[44] A "three layer" model was proposed (Figure 3a), in which the most immediate solvent molecules forms the strongest association with the ion and would likely to remain with the ion during its translational movement, while the solvent molecules far away from the ion maintain the undisturbed bulk structure. Somewhere between these two regions is an intermediate layer, whose bulk structure is broken by the coulombic field of the ion but their distance is not close enough to associate themselves with the moving ion. Nowadays we referred this inner and intermediate solvation layers as "primary" and "secondary" solvation sheaths, respectively. Such model actually assumes that sufficient solvent molecules are available for the ions to recruit, which does not hold true in super-concentration regimes due to the high salt/solvent ratios. The insufficiency of solvent molecules would lead to the disappearance of the bulk and secondary solvation sheaths, while the solvent molecules are forced to be shared by different ions. At extreme scenarios the anion-cation distance are so compressed that they enter the primary solvation sheaths of each other (Figure 3b-c). Such disruption of classical solvation sheath not only alters the local solvation environment around the ions, but also introduces liquid structures in long-range due to the aggregation of ions (Figure 3c-f).

3.1 Cation Solvation and Salt Dissociation

It is well established that better salt dissociation occurs with the stronger solvent-salt interaction and weaker cation-anion interaction. Ideal salt dissociation leads to free ions with negligible interionic attractions/expulsions. In reality, an electrolyte of higher fraction of free ions

is often obtained in the *salt-in-solvent* regime, which offers higher conductivity at a given viscosity. However, it is less clear if the same principle could be applied to the *solvent-in-salt* electrolyte when the population of solvent molecules is insufficient to fully coordinate all cations while separating cations from anions. In fact, it remains a question whether a significant fraction of free ions could exist in the solvent-limited *solvent-in-salt* regime. When a Li^+ cation can only access half of the solvent molecules needed to complete its first solvation sheath (i.e., solvent/Li=2), the fraction of free ions was found to be less than 3% for the acetonitrile (AN) solutions of $LiPF_6$, LiFSI, LiTFSI, $LiBF_4$, or $LiClO_4$.[45-47] Generally, in aprotic super-concentrated (3.5-5 M) electrolytes such as LiFSI in DME [48] or LiTFSI in AN,[49] the Li^+-coordination have a similar contribution from solvent and anion (2 solvents and 2 anions), as shown in Figure 7a for LiFSI in AN (AN/Li=2.67). The distribution of AN solvent and oxygen of TFSI around Li^+ is single peaked around two, with the majority of ions existing as ion-aggregates or ion-pairs with a very small fraction of free solvent separated Li^+. Therefore, the cation transport has to occur in these solvent-in-salt electrolytes either via the anion and solvent exchange or the charged cluster diffusion due to very small fraction of the solvent separated Li^+.

Replacing AN with water, which is a much stronger solvent compared to many aprotic solvents familiar to battery researchers, gives rise to a rather different Li^+-solvation sheath composition. At the same solvent/Li ratio of 2.67, a high fraction of the fully hydrated Li^+ was found in WiSE in MD simulations, despite that the first Li^+ solvation sheath cannot be fully completed due to the insufficient number of water molecules. Thus, in WiSE with 21 m of LiTFSI (H_2O/Li=2.67), a significant "disproportionation" in Li^+-solvation sheath occurs, leaving a high portion (~40%) of Li^+ exclusively surrounded by water molecules only, while the rest (>40% of Li^+) are mainly surrounded by TFSI (Figure 7a-b).[49] The stronger ability of water to solvate both Li^+ and anion compared to AN is responsible for such "disproportionation" in the local Li^+-environments, which in longer length leads to a heterogeneity on nano-scale (~1 nm) with *water-rich* and *anion-rich* regions, instead of an "average" solvation environments where solvent (water) and anion evenly distribute (Figure 7c). Counterintuitively, despite the stronger dissociation of LiTFSI in water than in AN, binding energy of the $Li^+(H_2O)_4$ is smaller than that for the $Li^+(AN)_4$, thus indicating that the anion-solvation by water vs. AN is important for the achieving salt dissociation.[49] The cluster-continuum quantum chemistry calculations of the Li-Anion dissociation predict the lithium salt dissociation in dilute solutions in good experiment with spectroscopic measurements,[50] however, they do not fully take into account the anion-solvation contribution and, therefore, should be used only for the same class of electrolyte with a similar anion solvation in order to provide consistent predictions.

When extending the solvation disproportionation to bivalent cations, an interesting distortion occurs due to the difference in cations' capability to interact with anions and solvent molecules. With 1m $Zn(TFSI)_2$ dissolved as minority salt in WiSE (21 m LiTFSI), the solvation sheath of Zn^{2+} was found to be solely occupied by anions (TFSI) without water presence, while a high fraction of free Li^+ were solely solvated only by water.[29] Apparently, Zn^{2+} loses its competition for water molecules to the majority cation Li^+.[29]

The "*salt-solvate*" electrolytes systematically studied by Watanabe and co-workers represent an intermediate concentration range, where the population of solvent molecules are just enough to complete the first solvation sheath of Li^+. Glymes of varying length (G*n*, where *n* in CH_3-$[CH_2CH_2O]_n$-OCH_3 shows the number of solvating oxygens) were used,[13-17; 20; 51] although other solvent molecules could also form salt-solvates, such as AN or carbonate esters studied by Henderson and co-workers.[18; 45; 46; 52;] In such systems, the presence of free solvent leads to both thermal and electrochemical instabilities as measured by mass loss at lower temperatures[15; 52] (Figure 4b) and degrading oxidative stability (Figure 4c).[13; 16] Weaker binding solvents such as THF<G1<G2<G3 (in the order of stronger solvation toward Li^+) also lead to the increased salt aggregation and higher fraction of free solvents in the super-concentration regime, thus degrading the oxidative stability of the salt-solvates.[13; 51]

The relative strength of the Li^+ interaction with solvents vs. anions in dilute solutions determines the extent of salt dissociation, ion aggregation and the correlation between cation and anion during ion transport. The later measure of the degree of ion uncorrelated motion was defined as "*ionicity*" by Watanabe et al., which can be probed via a combination of impedance and NMR techniques or conductivity and viscosity by relating molar conductivity of electrolyte (Λ_{imp}) to that calculated using ion self-diffusion coefficients (Λ_{NMR}) or the "ideal" KCl line based on a 1M KCl aqueous solution (Λ_{ideal}). An ideal electrolyte should have an ionicity of 1.0, reflecting no correlation between the cation and anion motion. It is realized in the completely dissociated dilute electrolyte, and such ideal behavior can only be reached in good solvents at very low concentrations.[53] If ionic solvation is poor, the opposite behavior is observed with the ion aggregation increasing and the cation-anion motion becoming more correlated as salt concentration decreases.[54]

In the salt-solvate electrolytes there is a strong inverse dependence of the extent of ion uncorrelated motion (ionicity, a dynamic property) and a fraction of free solvent (structural property) as shown in Figure 8a. The lower the fraction of free solvent, the more solvent participates in the Li^+ solvation, dissociating salt and making ionic motion less correlated due to electrostatic screening. The ion correlation and aggregation trends for the glyme-based solvated salts obtained from dynamic and spectroscopic measurements (Figure 8a) are similar to the trends deduced from the previous study of phase behavior and crystalline solvates for $(glyme)_n$-LiX mixtures by Henderson:[18] $LiN(SO_2CF_3)_2$ (TFSI), $LiAsF_6$ < $LiClO_4$, LiI < $LiBF_4$ < $LiCF_3SO_3$ < $LiNO_3$, LiBr < $LiCF_3CO_2$. Similar trends were reported for "ionicity" in 0.75 M γ-Butyrolactone (GBL): $LiPF_6$ ≈ LiTFSI ≈ LiBETI > LiBF4 > LiOTF.[55] There is also a very good correlation between the "ionicity" ($\Lambda_{imp}/\Lambda_{NMR}$) in the glyme salt-solvates and the Li^+ solvation number in the EC-based electrolytes at the lower salt concentration (EC/Li=10) as shown in Figure 8b, indicating that the similar trends for salt dissociation and ionic correlation seem to hold for these different solvents (glyme and EC).

While the more associated salts result in lower ionicity (higher correlation of ion motion) and higher fraction of free solvent, the higher ionicity does not necessarily reflect high ion dissociation as salt concentration increases towards the solvated salt regime. Approaching super-

concentration, counterintuitively, leads to increased ionicity ($\Lambda_{imp}/\Lambda_{NMR}$) in (Figure 8c), despite increasing ion pairing and aggregation that occur simultaneously.[51] Maximum ionicity is reached at a fixed stoichiometric ratio of ether units and Li^+ (EO/Li^+~4), which happens to be a typical Li^+ solvation sheath structure in ether-based solvents. We attribute it to the anti-correlation of the $Li^+(EO)_4$ solvate and anion-motion as required by the conservation of momentum in this highly dissociated electrolyte with little free solvent. Similar high ionicity (0.6-0.8) was found for the highly concentrated WiSE, which is significantly higher than the fraction of the solvent separated Li^+ that is only 0.4.[49]

3.2 Anion Solvation

The solvation of anions is highly system-specific. In most commonly-used non-aqueous solvents, anions are typically not, or at least very little, solvated as compared with cations.[56] This is owing to the facts that most non-aqueous solvent molecules are better electron donors rather than acceptors, and that anions are much larger than cations, leading to much smaller coulombic interactions with the solvent. Typical anions PF_6^- and FSI^- have been found via liquid secondary ion mass spectra (SIMS) to be much less strongly solvated by either carbonate or ether solvents than their counterion (Li^+),[56; 57] where a well-defined solvation sheath no longer exists. However, this cation-preferred solvation behavior would change when the solvent molecules become water, whose bipolar nature had been well established. It is this water-TFSI association that further assists in the LiTFSI salt dissociation leading to the Li^+-solvation shell disproportionation that is directly responsible for the long-range (~1.0 nm) heterogeneity network found in WiSE mentioned above.[49] The question remains unanswered regarding whether such a structure exists in non-aqueous electrolytes at super-concentration regimes, but obviously the weak solvation behavior of anions makes it much more difficult to dissociate lithium salt as need to form the water-rich and salt-rich nano-domains.

4. Ion Transport

In classical Bernal-Fowler Model, the solvent molecules in a primary solvation sheath are considered “permanently” attached to the ion, hence the sheath composition should remain static during the ionic movement.[44] While these solvent molecules indeed have stronger binding with the ions than the molecules in secondary and bulk regions, the stability of the sheath structure is only true in the time scale of pico- to nano-seconds, as evidenced by the fact that these different solvent molecules can only be differentiated using ultra-fast spectroscopy. Furthermore, MD simulations indicate that residence time of Li^+ with solvent molecules could be longer or shorter than the Li^+-anion residence times depending on the salt, solvent and concentration.[58-60] Hence, with the exception of dilute electrolytes based on a good solvent or aqueous electrolytes, one can almost never rely exclusively on the free cations (fully solvent separated from anions) to achieve high ionic conductivity. Even one of the most dissociating salts such as LiTFSI in dilute regime (solvent/Li=20) show the degree of uncorrelated motion (“ionicity”) between 0.1 and 0.64 for 14

solvents of interest to batteries, which is significantly below 1 for the fully dissociated and uncorrelated system.[61]

4.1 Ion Transport: Vehicular vs. Structural

The manner of ionic transport across the electrolytes can be described as either *vehicular* or *structural*. In the former, the solvation sheath travels with the solvated ion, while in the latter, the ion hops via a serial ion association-dissociation process if the solvating sites are immobilized (as in solid state electrolytes), or via frequent exchange of solvent molecules (when these solvent molecules are mobile themselves).[58-60; 62; 63] Of course, these scenarios represent two extremities. An ion could travel simultaneously in both manners, because, given the transient stability of solvation sheath, ions would eventually experience complete replacement of the inner solvent members in their primary solvation sheath.

The relative contributions of the vehicular and structural (solvent or anion exchange) modes to the cation diffusion can be quantified via a ratio of the averaged distance a solvent (or anion) moves together with a cation to the size of the solvent (or anion). When a cation moves multiple solvent sizes before it exchanges the solvent molecules in its coordination shell, the transport mechanism is largely vehicular as observed for the Li^+ in glymes and aqueous electrolytes in both solvent-in-salt and solvated salts-regimes if the salt is strongly dissociated such as LiTFSI.[49; 58; 64] The strong chelation of Li^+ by multiple ether oxygens make the Li^+-transport in ether-based electrolytes almost exclusively vehicular, as Li^+ moves around three solvent sizes before it exchanges all solvent molecules for 1,2-dimethoxyl ethane (DME) and pentaglyme (G5, denoted as EO_6 in Figure 9a).[58] Hence, a Li^+-glyme complex largely travels in its entirety without disruption of the solvation sheath. Such inference was supported by experimental observation that the diffusion constant ratio $D_{solvent}/D_{Li^+}$ approaches 1.0 in glyme-based electrolytes as concentration approaches the solvated salt regime.[51; 65] When an oligoether chain length increases past 5-6 repeat units needed to solvate a single Li^+ to 54 repeat units, the Li^+-transport mode becomes structural, as represented by Li^+ moving along the polymer chain and hopping between the polymer segments (also Figure 9a). The weaker Na^+-glyme binding as compared to Li^+-glyme and the larger size of the Na^+-solvation sheath result in a switch of the transport mechanism from being primarily vehicular to structural with frequent solvent exchange for DME doped with NaFSI and NaTFSI.[64; 66] A similar trends was observed in the ionic liquid-based electrolytes, where a dominance of the vehicular contribution over structural diffusion increased with increasing the cation-anion binding energy in the order: $[Zn(TFSI)]^+ > [Mg(TFSI)]^+ >$ LiTFSI > NaTFSI.[62]

Unlike glymes, a similar contribution of the vehicular and structural was observed for the carbonate-based electrolytes (Figure 9a) in salt-in-solvent and solvated-salts regimes (up to 3 M) and in the solvent-in-salt regime for the AN-based electrolytes.[58; 59; 67; 68]. Figure 7b demonstrates how the Li^+-solvent and Li^+-anion exchange varies with salt concentration by plotting the average distances a Li^+ travels before exchanging all its solvents, TFSI anion (N of TFSI) and oxygens of TFSI. In the salt-in-solvent regime, the Li-AN move together slightly less than two AN sizes using 5 Å as an estimate of the AN size along the longest dimension. In the solvent-in-salt regime (AN/Li=2), the Li^+ exchanges AN as its moves slightly less than one size of AN, thus suggesting

that the solvent exchange becomes dominant. A relatively strong binding of the Li^+ to $TFSI^-$ vs. AN results in a slower exchange rate of Li^+ with TFSI anions than with AN solvent, thus, in dilute solutions, the LiTFSI ion pairs move largely via the vehicular mechanism. Multiple exchanges of the Li-O(TFSI) occur before the Li-N(TFSI) dissociates and the anion completely leaves the Li^+. This picture is consistent with suggestion from Yamada et al. that super-concentration might disrupt the vehicular-dominance manner, leading to a repeated ion association/dissociation process, which is a form of distinct structural diffusion.[22] However, one needs to keep in mind that the structural vs. vehicular contributions could be different for the solvent and anions.

Highly viscous and relatively large sulfolane (SL) solvent has two closely spaced solvating oxygens in the $–SO_2$ group (Figure 9c) allowing a Li^+ to exchange them at the same time scale as it moves a size of the SL molecule.[69] A similar Li^+ and solvent diffusion was observed in the salt-in-solvent regime (SL/Li=8.33), while in the solvent-in-salt regime (SL/Li=2.56) the Li^+ diffusion was more than 50% higher than SL diffusion from MD simulation predictions[69], which were confirmed by pfg-NMR measurements.[69; 70] A significantly faster Li^+ diffusion than solvent is rare, as typically the Li^+ diffusion is lower than that for the solvent in the salt-in-solvent regime, with few exceptions where it become comparable or only slightly faster.[13; 17; 61; 71]

We summarize main factors influencing the relative contributions of vehicular and structural diffusion to the metal cation transport in Figure 9c. A strong cation-solvent binding, low solvent viscosity (DME or AN) and small solvent size (water) favor the vehicular mechanism, which could switch to structural diffusion as salt concentration increases. On exception is water: even in the water-in-salt regime (21m LiTFSI, H_2O/Li=2.67), a high fraction of the fast moving solvent-separated $Li^+(H_2O)_4$ indicated prevalence of the vehicular mechanism as the $Li^+(H_2O)_4$ moved multiple sizes of water molecules before the Li^+ exchanged its solvation shell.

An alternative descriptor related to ionic transport is the Walden analysis, where the correlation between molar conductivity (concentration-normalized conductivity) and viscosity is compared, and a linear relationship in a given concentration range may indicate a well-dissociated electrolyte. According to Yamada et al., the Walden plot of their "*hydrate melt*" electrolyte, which bears close similarity to WiSE, reveals a pronounced cation-anion decoupling behavior, benefited from the well-dissociated lithium salts in H_2O and strongly suggesting an ionic hopping process [50, 51]. From an electrolyte performance perspective, it remains unclear which mode of diffusion is desirable, although Bedrov et al., via molecular dynamics analysis, suggested that a more structural diffusion may allow a higher true transference number.[63]

One important ramification of the liquid structure with nano-heterogeneity is the fast Li^+ transport, which is enabled by the high fraction of free Li^+ via a vehicular motion through the *water-rich* region.[49] Existing as a 3D percolating network in WiSE, and experimentally evidenced by small angle neutron scattering (SANS, Figure 7d),[49] this pathway for fast Li^+ transport originates from the local solvation structure, i.e., the disproportionation in Li^+-solvation sheath structure. Since anions are relatively immobilized by the *anion-rich* phase, the transport of those Li^+ is preferred, as evidenced by the high Li^+- transference numbers as measured by pulse-field NMR.

4.2 Ion Transference Number

Besides ionic conductivity, *ion transference number* (t_+) is an equally important descriptor for ion transport. While the former defines the overall capability of an electrolyte to provide ionic current, the latter describes the "quality" of such capability, because it quantifies the portion contributed by each ionic species to the overall ionic current, given that for an electrochemical device, only the portion of the current carried by the ions essential to the cell reactions matters. A high t_+ for essential ions implies high rate capability for the resultant electrochemical device, which minimizes the bulk electrolyte resistance under the condition of fast charge or discharge.

In dilute electrolytes based on "good solvents", the ions are effectively screened from their counterions, hence their movements should be considered uncorrelated to interionic effects, and the cation transference number could be approximated using self-diffusion coefficients obtained from MD simulations or pfg-NMR measurements:

$$t_+(ideal) = \frac{D_+}{D_+ + D_-} \quad (1)$$

This approximation, however, breaks down even in dilute regimes whenever there is strong interionic association, examples of which include strongly dissociated salts in poor solvents (such as alkylpyrrolidinium/TFSI in DMC), where ion correlation increases with decreasing salt concentration, in a complete reversal of what expected from a well solvated electrolyte[54] and other strongly aggregating electrolytes even at low salt concentrations such as fluoromethane-THF/LiTFSI[72] or $LiCF_3CO_2$ in AN.[73] Thus, eq. 1 should be applied with caution for those scenarios where interionic attraction cannot be ignored.

A convenient formalism for calculating t_+ was suggested by Wohde et al.,[74] who, based upon Onsager reciprocal relations combined with linear response theory, considered two important regiments characterized by their parameter β: (1) a strongly coupled ion and cation motion due to ion pair formation ($\beta \rightarrow 1$) that reduces t_+; and (2) an anti-correlation of the positive and negatively charged current contributions due to Li^+ moving together with a bulky solvation shell in the opposite direction in order to preserve momentum, thus creating an anticorrelation ($\beta \rightarrow -1$).[63] Because Li^+ mass is often significantly lighter than solvents and anions, it is reasonable to assume that electrolyte center of mass should be conserved and apply this formalism to equilibrium MD simulations to extract t_+.

Dong et al. demonstrated that the t_+ for the salt-solvate electrolyte LiTFSI/G4 (1/1) under anion-blocking conditions can be much lower than t_+(ideal).[54] They reported that the mobility of Li^+ and $TFSI^-$ is similar, leading to $t_+(ideal) \approx 0.5$. However, MD simulations and analysis of experiments showed that the anti-correlated motion in combination with anion blocking condition results t_+ being only (0.02–0.06). Similar result was generated by our simulations (Figure 10). Such behavior is related to the momentum conservation constraint and inability of G4 molecules associated with the Li^+ to support the momentum exchange between ions. This finding indicates

that such solvated salt electrolyte cannot support the charge-discharge rates expected from t_+(ideal). In order to overcome this detrimental effect for battery applications, Dong et al. [54] suggested to improve the momentum exchange so that anti-correlated motion of ions could be minimized, which can be realized by (1) diluting electrolyte with additional solvent molecules that are not complexing with Li^+ ions; or (2) decreasing the residence time for solvent molecules near Li^+ so that the ionic transport mode is switched from vehicular to structural. The latter can happen when the short-chain glyme molecules or carbonates are used.[58] In both approaches, solvent molecules facilitate momentum exchange in the system and therefore the momentum conservation in the system can be accomplished without strong dynamic correlations between ions.

A significant increase in t_+ from 0.02 to 0.19 indeed realized when a longer glyme G4 is replaced with a shorter glyme (G1, DME), and a smaller salt (LiFSI) is introduced as a bi-salt electrolyte (Figure 10). The faster Li^+ exchange as compared to longer glymes,[58] and shorter residence time of LiFSI vs. LiTFSI by a factor of two at room temperature partially switched the Li^+-transport mechanism from the vehicular to structural, resulting in much higher t_+ despite higher concentration of salts (3.4 M LiTFSI-LiFSI in DME vs. 2.8 M LiTFSI in G4). High contribution of the Li^+-solvent exchange and faster Li^+ than solvent diffusion lead to not only t_+ (ideal) but quite unusually to t_+ being higher than 0.5 for the SL/LiFSI electrolyte. Unlike a strongly decreasing t_+ with increasing salt concentration for the G4-LiTFSI electrolyte, an inverse trend of a slightly increasing t^+ observed for SL/LiFSI during additional analysis of MD simulations.[69] Using small and light water molecule compared to the much larger and heavier glymes present an alternative strategy to improving t_+ compared to t_+ (ideal) in the superconcentrated regime. Preliminary results indicate that, even in the most concentrated regime (21 m LiTFSI), the presence of strong solvent water still manages to ensure a much weaker anticorrelation with the $TFSI^-$ anions, as evidenced by the t_+ that is only slightly decreased as compared with t_+ (ideal).

Thus, the effect of super-concentration on t_+ is by no means monotonous. Extremely low t_+ occurs with the formation of large Li^+-solvates, as in the case of salt-solvates by ether solvents. Although these solvated species are well separated from anions by the strong solvating molecules, the long residence time of the solvents make the solvated Li^+ rather clumsy in motion. Introducing ligands that could be rapidly exchanged, such as light and strong solvent (water) or strongly dissociating anion (FSI) could lead to t_+ even higher than t_+ (ideal).

As salt concentration decreases in good electrolyte, one expects t_+ to approach t_+ (ideal) due to decreased ion correlation as solution becomes more dilute. However, a recent report that the strong ion correlations lead to t_+ being higher than t_+ (ideal) at low salt concentration fluoromethane (FM):THF-0.5 M LiTFSI electrolyte is quite intriguing.[72] This large and positive deviation from non-ideality is clearly due to ion aggregation, specifically due to formation of the large negatively charged slow moving clusters containing an excess of $TFSI^-$ and solvent separated Li^+ solvates that diffuse fast in a low viscosity FM solvent. Despite similar average self-diffusion coefficients for Li^+ and $TFSI^-$, the diffusion of the solvent separated Li^+ is 2-2.5 times faster than the average diffusion coefficients of all Li^+ and $TFSI^-$ anions. The much higher fraction of free Li^+ as compared to free $TFSI^-$ indicates a high contribution of Li^+ to the electrolytic conductivity compared to anion contribution that move slower and essentially do not exist as free ions. Experimentally, a slightly smaller value of

t^+=0.79 was measured using the potentiostatic polarization method but it indicates experimentally that t^+ for low salt concentration could be above 0.5, albeit it is unusual.

5. Interfacial Structure and Interphasial Chemistry

Among the "unusual" properties brought by super-concentration, perhaps the most important is the new interphasial chemistries that differ from the non-concentrated systems. Such new interphases are already recognized as the key to enable electrochemistry at extreme potentials, and examples include the super-concentrated ethers, sulfone, sulfoxide, nitriles and even water, which form protective interphases on various electrode materials and make them reversibly functional at potentials otherwise impossible. All these new interphases now bear chemical signatures from the anions instead from the solvent molecules, unlike dilute electrolytes whose interphasial chemistry are primarily dominated by the reduction or oxidation of solvent molecules. It was this new chemical reliance of interphase on anion instead of solvent molecules that lifts the many traditional confinements imposed on electrolyte design, the most conspicuous of which is ethylene carbonate (EC), the indispensable solvent in electrolytes for any LIBs manufactured nowadays, primarily because of its key role in forming interphase on graphitic anode [55].

Although a correlation has been established between Li^+-solvation sheath and the interphase assuming a transition state of Li^+-solvent co-intercalation into graphite[56], predicting interphasial chemistry has been, and still is, challenging. In a more general context, it is reasonable to assume that before the potential of a certain electrode reaches the threshold value of "breaking down" electrolyte components, where *interphasial* chemistry starts, there should be already an *interfacial* structure existing at the so-called inner-Helmholtz layer. This self-assembly of electrolyte components, enriched in certain components while deprived of the others, should be the immediate parental entity that dictates the eventual interphase. Hence, understanding its chemical composition and structure might provide the key knowledge to predict interphase chemistries.[32; 72; 75-78]

Consider a graphitic anode in a typical carbonate electrolyte (~1.0 M $LiPF_6$) is being charged for the first time. At the moment its surface is free of any interphase, but an interfacial assembly was already built up when it was in contact with electrolyte. As the graphite is negatively polarized, this interfacial assembly at inner-Helmholtz layer should gradually become enriched with Li^+, [79] along the solvent molecules in the Li^+-solvation sheath. These solvent molecules are made susceptible to reduction more than other species, because of their close proximity to anode surface and the activation of the bonds within them by Li^+. Meanwhile the anions would be pushed away to the outer-Helmholtz layer by the anode surface due to increasing negative charges, forming an electric double layer structure with distinct cation-rich and anion-rich regions (Figure 11a).

Such an inner-Helmholtz structure will be disturbed by the change of the salt concentration in the electrolyte. The super-concentration would compress the thickness of the inner-Helmholtz layer and force the anion to approach the anode despite the coulombic expulsion (Figure 11b). The

consequence of such an interface with higher anion population and Li-Anion aggregation certainly increases the chances of anion-reduction due to excess electron stabilization when the anion is coordinated with one or multiple Li^+ or other cations [25; 27; 28], which often increases the reduction potential of anions. Thus, super-concentration provides a viable option to manipulate interphasial chemistry by switching its potential source from solvent molecules to anions. [22; 23; 25; 27; 28; 42; 69; 80-83]

Similar process would happen on the cathode surface. MD simulations revealed that anion concentration increases in the inner-Helmholtz layer as an electrode becomes positively polarized. [79] When electrolytes are based on mixed solvents, such as the typical formulations used in commercial LIBs, a preferential partitioning of EC vs. DMC or other linear carbonates at both negative and positive electrodes increases its opportunity of participating SEI and CEI formation [79]. Both solvent and anions are found in the inner-Helmholtz layer next to cathode surface when the salt concentration is ~1.0 M, [79] while super-concentration or ionic liquids completely populate the inner-Helmholtz layer and expel all solvent molecules away from the cathode surface, screening them from possible oxidation. [52; 76-78] The anion structure also plays a role in deciding if preferential adsorption could occur. For example, MD simulations[77] found that TFSI seems to be favored over trifluoromethane sulfonate (OTf) during positive electrode polarization from potential of zero charge, which has been confirmed by the surface-enhanced IR spectroscopy [78].

Compared with the cathode, which attracts anions due to its positive-charged surface, the intrinsic repulsion of anions by the negatively-charged anode creates the so-called "*cathodic challenge*", which makes the anion-derived SEI more challenging than CEI. [32] When an extremely negative potential is applied, even the super-concentration cannot overcome the strong repulsion in order to populate the anode surface with sufficient anions required for SEI formation. Cationic species such as $Li^+(H_2O)_n$ in the WiSE would eventually appear at the anode surface, resulting in water reduction and preventing the emergence of any SEI.[77] This difference between the anode and cathode surfaces in their preferred inner-Helmholtz structure constitutes the fundamental reason for the strong "*positive bias*" observed for the expanded electrochemical stability window for WiSE and its derivatives (hydrate melt, water-in-bisalt, etc.), leaving anode as the most challenging component to stabilize in aqueous electrolytes.[34]

In their initial publication, Suo et al. described the chemical composition of the aqueous SEI formed in WiSE as neat LiF, which was confirmed by various spectra including chemical analysis via EDX under TEM, XPS[25] as well as SIMS.[75] This conclusion seemed to be reasonable, because LiF is the least soluble lithium salt in water[84], which makes it an excellent candidate as component of aqueous SEI. This argument was strengthened later on in the sodium version of WiSE, where the SEI identified on the surface of the cycled anode seems to be even more pure NaF with clear lattice structure matching the crystal database. In a more detailed mechanism study, Suo et al. further established the correlation between the hydrogen evolution and the LiF-formation during the first charging cycle,[75; 85] while sequential bombardment of the formed SEI by Ga^{3+} revealed the presence of minor Li_2O and Li_2CO_3 in addition to the major component LiF. They

attribute the formation of Li_2O and Li_2CO_3 to the reduction of water and the trace amount of CO_2 dissolved in WiSE.

More recent studies challenged the SEI formation mechanism in WiSE that has been centered on direct electrochemical reduction of TFSI. Dubouis et al. proposed that the free, unbound water molecules plays the key role, which re electrochemically reduce to hydroxide accompanied by hydrogen evolution during the first charging. [84] TFSI then undergoes nucleophilic attack by hydroxide, chemically decomposes and lead to LiF or NaF deposited on anode surface as eventual interphasial components. Lee et al. even claimed that an aqueous SEI does not necessarily require the anion to provide chemistry source. By using a super-concentrated (17 m) electrolyte based on $LiClO_4$, they showed that interphases were formed with Na_2CO_3 and NaOH as the main component, without apparent participation from anion.[86] Thus, Lee et al. attributed this new interphasial chemistry to the oxygen and CO_2 dissolved in the WiSE, which had been recognized earlier by Suo et al. but were not thought to be the chemical basis for an interphase.[25] Zheng et al. further argued that the main contribution to the expansion of electrochemical stability window could be the result of neat kinetic barrier for a water molecule to free itself from a polymer-like local structure $[Li^+ (H_2O)_2]_n$ in WiSE.[87] Given the fundamental importance of this topic, more debate and intensive research are likely.

Finally, in order to overcome the cathodic challenge, so that an electrochemical stability of >4 V could be established for aqueous electrolytes, Yang et al.[32] leveraged the two characteristics of fluorinated ethereal compounds: (1) they are hydrophobic by nature, so they can effectively shield the anode surface by pushing water molecules away from the inner-Helmholtz layer before interphase formation; and (2) they are active toward electrochemical reduction like their carbonate counterparts FEC or FEMC, which generates LiF as well as numerous fluorocarbon species that a new interphase could use as chemical building blocks. Under the protection of this new interphase, graphitic anode can be lithiated to its 1st stage, delivering a specific capacity of ~300 mAh/g and enabling a 4 V class aqueous Li-ion battery for the first time. This technique provides the foundation for high voltage aqueous battery chemistries that could eventually compete with state-of-art Li-ion batteries in terms of energy densities.[33]

6. A New Horizon

Super-concentration does not just represent simply dissolving more salt in electrolytes. It opens up a brand-new horizon, not only for electrolyte materials but in broader context for solution chemistries, electrochemistries and processes. By drastically changing the primary solvation environments of ions, super-concentration induces the emergence of a sequence of unusual properties and behaviors, such as long-range liquid structures, preferential ion transport, interfacial structures as well as interphasial chemistries. As the interest in this new approach intensifies, more systems are developed, and in-depth understanding is achieved aided by advanced characterization and computational tools, we expect that more unusual properties beyond the current scope of electrochemistry and energy storage research will be discovered.

Acknowledgements

This work was supported as part of the Joint Center for Energy Storage Research, an Energy Innovation Hub funded by the U.S. Department of Energy, Office of Science, Basic Energy Sciences. The authors thank Dr. Marshall A. Schroeder (ARL) for discussions.

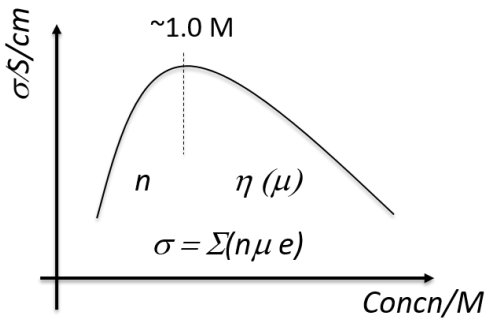

Figure 1. The compromise between ionic carrier number (n) and solution viscosity (η) creates the maxima in ionic conductivities, which occurs in the neighborhood of 1.0 M for most non-aqueous electrolytes.

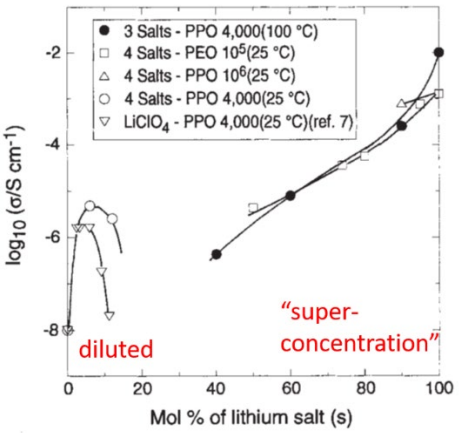

Figure 2. The "polymer-in-salt" approach represents an early attempt to breach the concentration confinement imposed by n-η compromise. Here the polymer serves as the macromolecular solvents for lithium salts. Reprinted with permission from Ref. 9 Copyright 1993 Springer Nature.

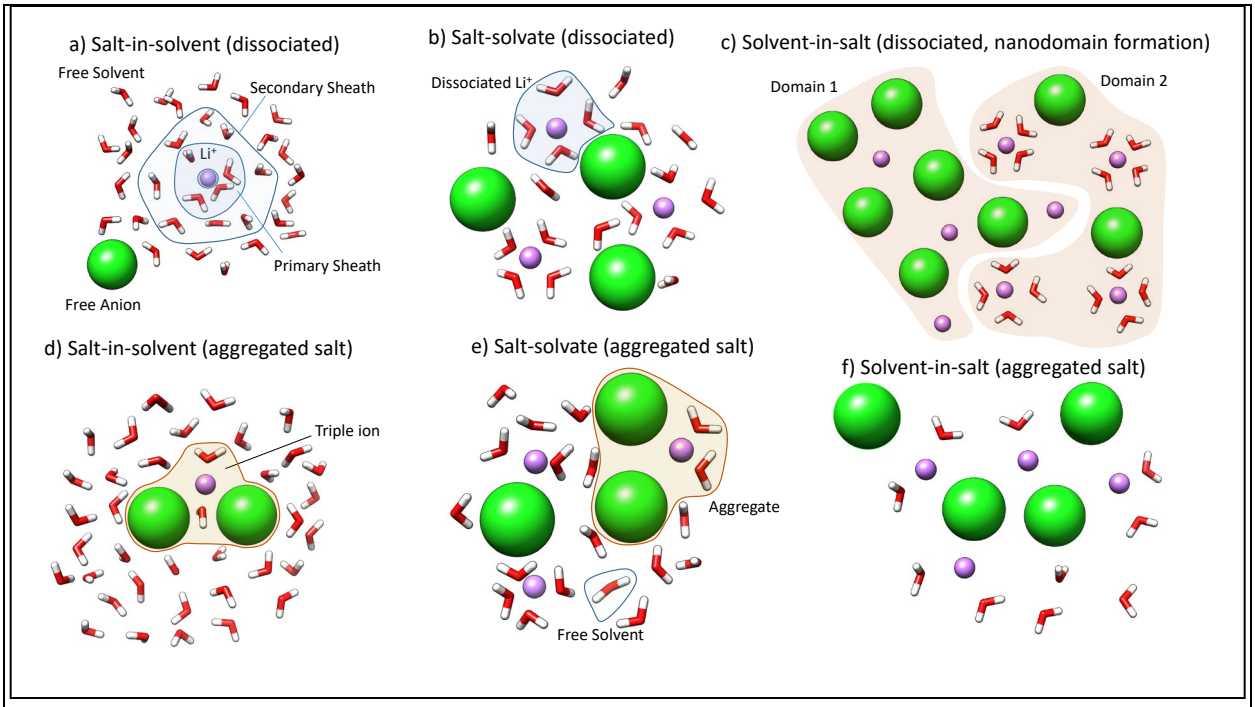

Figure 3. Schematic representation of three salt concentration regimes for the dissociating (a-c) and aggregating (d-f) salts: (a,d) ion solvation sheath in "diluted" electrolytes with the three layers: the primary, secondary solvation sheaths and the bulk free solvent, while the anion remains little solvated (green); and (b-c, e-f) the solvation structure in super-concentration regime, where the primary solvation sheath is disrupted by insufficiency of solvent molecules, and the presence of anions in the close vicinity of central cation. The shared solvent molecules constitute multiple interpenetrated solvation sheaths.

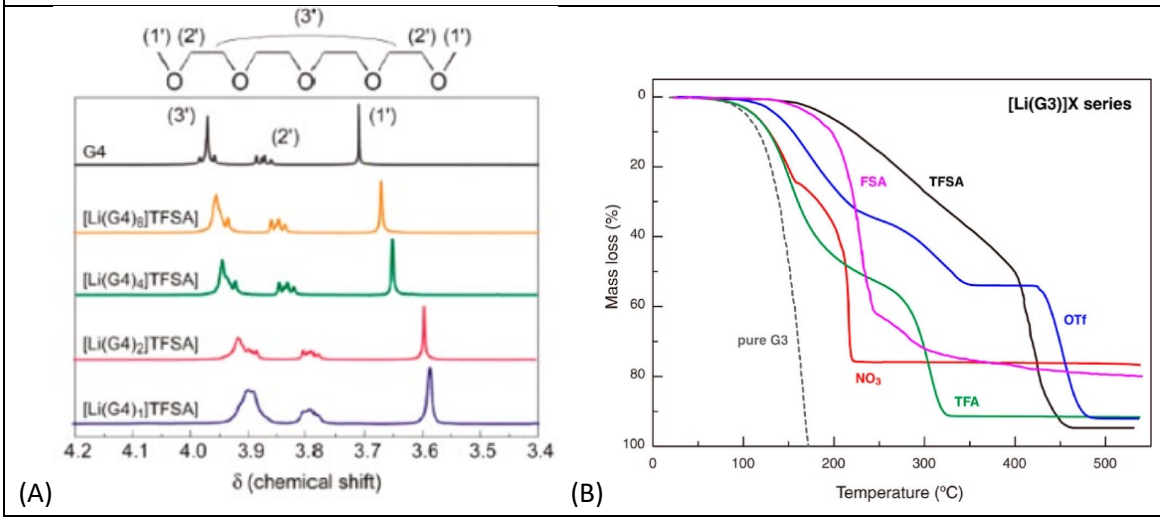

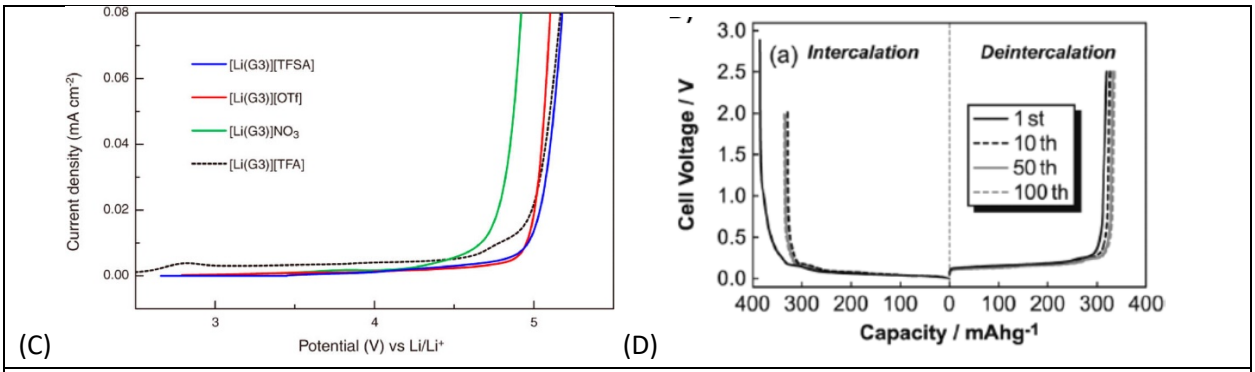

Figure 4. The unusual thermal, transport and interfacial properties found at super-concentrations for glyme-based electrolytes.[13; 16] (A) ^{1}H NMR spectra for pure glymes in solvated salts;[16] (B) Thermogravimetric analysis of LiX(G3) solvate-salts.[13] (C) Linear sweep voltammograms of [Li(G3)]X at scan rate 1 mV s^{-1} and 30 °C on Pt working electrolyte with Li metal as counter and reference;[13] (D) The charge-discharge profiles of graphite anode in TG-LiFSI electrolyte.[13; 20] Reprinted with permission from[13; 16] Copyright 2011, 2012 American Chemical Society.

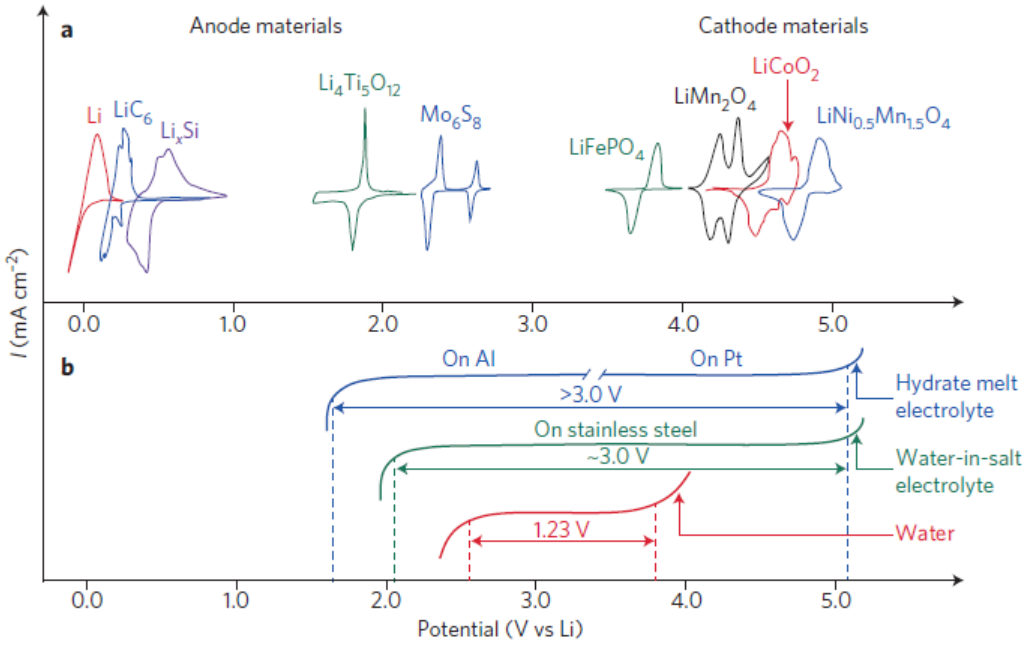

Figure 5. Extended electrochemical stability windows of aqueous electrolytes via super-concentration. (a) The redox potentials of major anode and cathode materials: Li-metal, Mo_6S_8, $Li_4Ti_5O_{12}$, $LiMn_2O_4$, $LiFePO_4$, $LiCoO_2$, and $LiNi_{0.5}Mn_{1.5}O_4$; (b) Redox reactions of water molecules at pH = 7 evolves hydrogen and oxygen at anode and cathode surfaces, respectively, giving rise to a thermodynamic stability window of 1.23 V, whereas super-concentration (21 mol kg–1 LiTFSI in WiSE, and 27.8 mol kg–1 LiTFSI+LiBETI in the hydrate melt electrolytes) significantly expands windows to larger than 3.0 V. Reprinted with permission from Xu et al [34] Copyright 2016 Springer Nature.

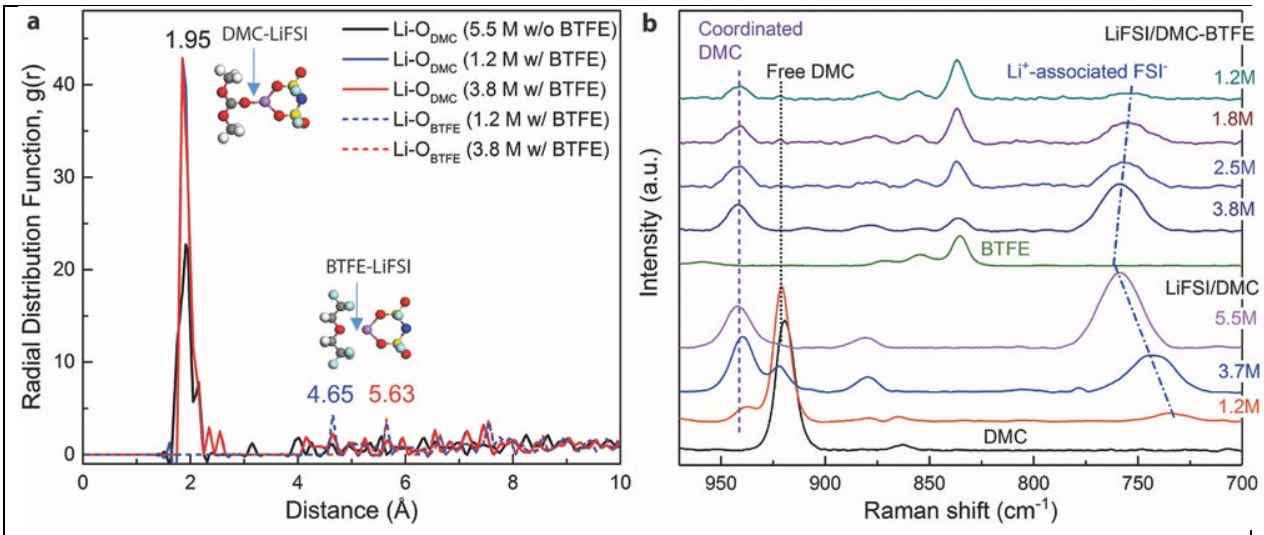

Figure 6. Localized super-concentration by non-solvent: (a) Radial distribution functions of Li–O_{DMC} and Li–O_{BTFE} pairs calculated from the last 5 ps of 15 ps AIMD simulation trajectories at 30 °C in electrolyte consisting of LiFSI dissolved in mixture of DMC and a fluorinated ether (BTFE). Insets shows the structures of DMC–LiFSI and BTFE–LiFSI solvent-salt pairs. Due to much shorter AIMD run length (15 ps) compared to the average time it takes a Li^+ to renew its solvation sheath in similar electrolytes (~10^2 ps) [68] the resulting solvate structure should be considered "quasi-equilibrated".[35] (b) Progression of Raman spectra with different salt concentrations in pure DMC and various DMC/BTFE mixtures. Reprinted with permission from Chen et al.[35] Copyright WILEY-VCH 2018.

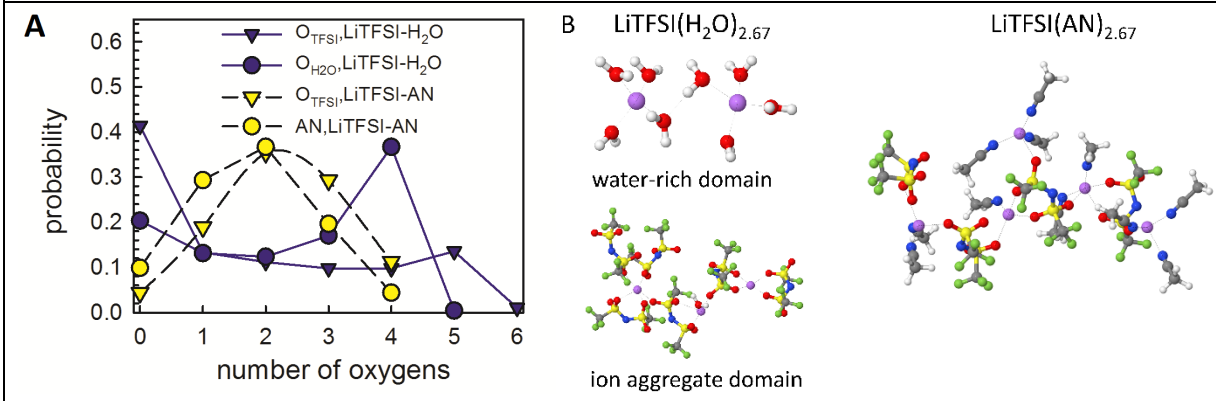

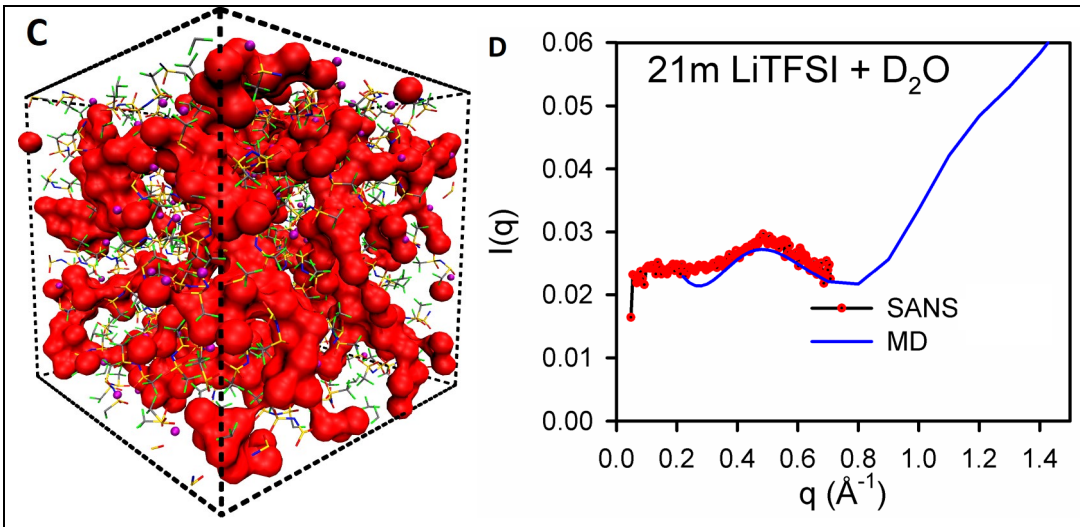

Figure 7. (A) A distribution of solvent and oxygen of TFSI around Li^+ (<2.8 Å) in H_2O/LiTFSI=2.67 (4.94 mol L^{-1}, 20.8 mol $kg_{solvent}^{-1}$) (dark blue) and AN/LiTFSI=2.67 (3.6 mol L^{-1}, 9.14 mol $kg_{solvent}^{-1}$) (yellow), respectively. Probability for a Li^+ to have zero number of O_{TFSI} corresponds to the solvent separated cations. [49] (B) The most probable lithium solvates extracted from MD simulations of LiTFSI in H_2O and AN at the solvent/Li=2.67 salt concentration. (C) A snapshot of the MD simulation box for 21m LiTFSI in H_2O with the $Li^+(H_2O)_n$ domain shown as a red isosurface, while the $TFSI^-$ anions shown as ball-stick model. [49] (D) Structure factor for 21m LiTFSI in D_2O from MD simulations and SANS measurements. [49] Reproduced with permission. Copyright American Chemical Society, 2017.

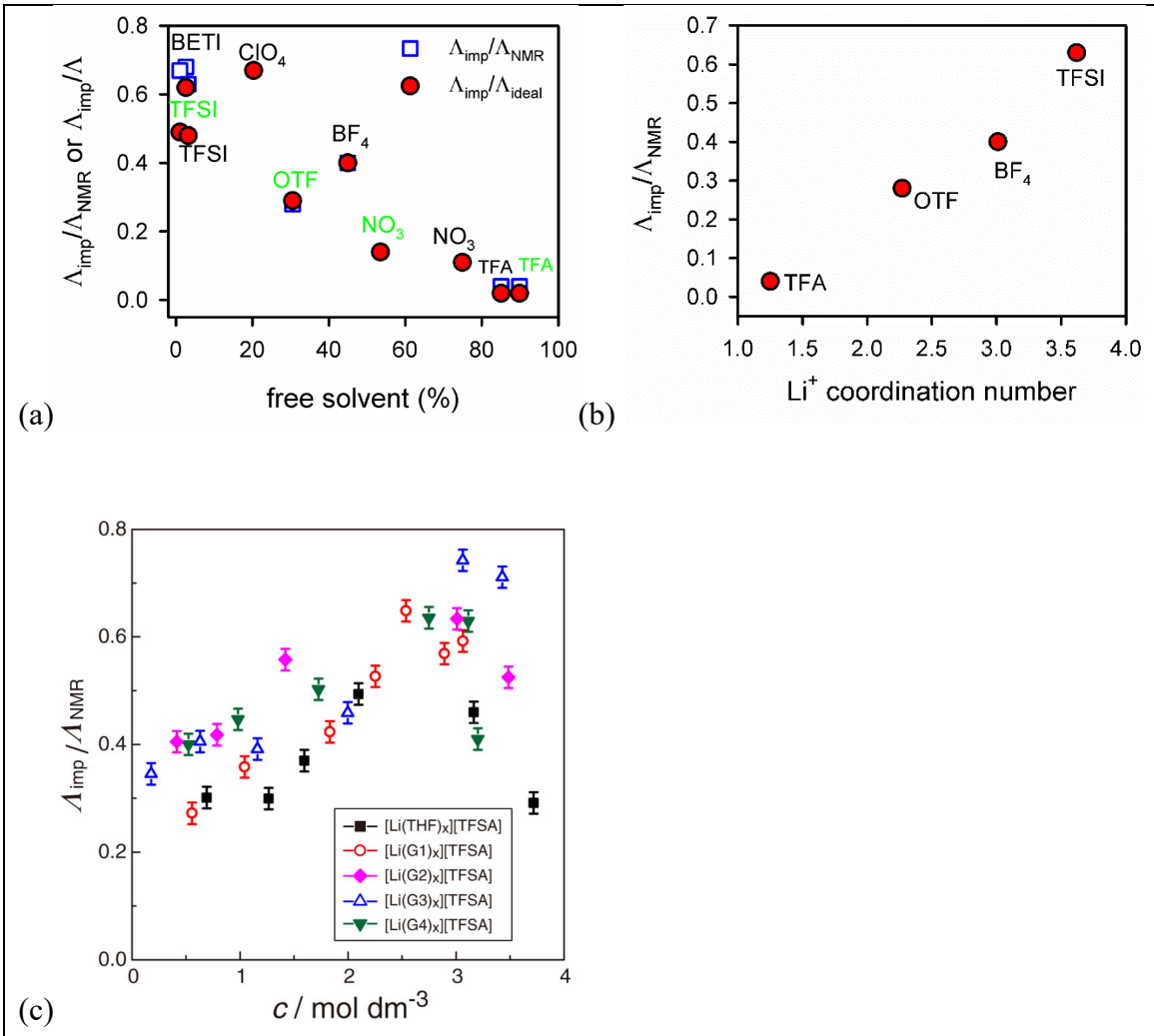

Figure 8 (a). A relation between a fraction of free solvent and degree of uncorrelated ion motion (often called ionicity) for G3(Li)Anion (green) and G4(Li)Anion solvated salts. Anion abbreviations: $N(SO_2CF_3)_2$- (TFSI), $CF_3SO_3^-$ (OTF), $N(SO_2CF_2CF_3)_2$- (BETI), CF_3CO_2 (TFA). Compiled from NMR, conductivity and viscosity data from ref.[13] and Raman measurements.[88] (b) the degree of ion uncorrelated motion for Li(G4)[TFSI,BF_4,TFA], Li(G3)ClO_4 solvated salts[13] plotted vs. the Li^+ solvation number at EC/Li=10) as extracted from Raman spectroscopy.[89] (c) Ionicity ($\Lambda imp/\Lambda_{NMR}$) at 30°C for [Li(glyme or THF)$_x$][TFSA] mixtures as a function of concentration. [51] Reproduced with permission from.[51] Copyright 2014 American Chemical Society.

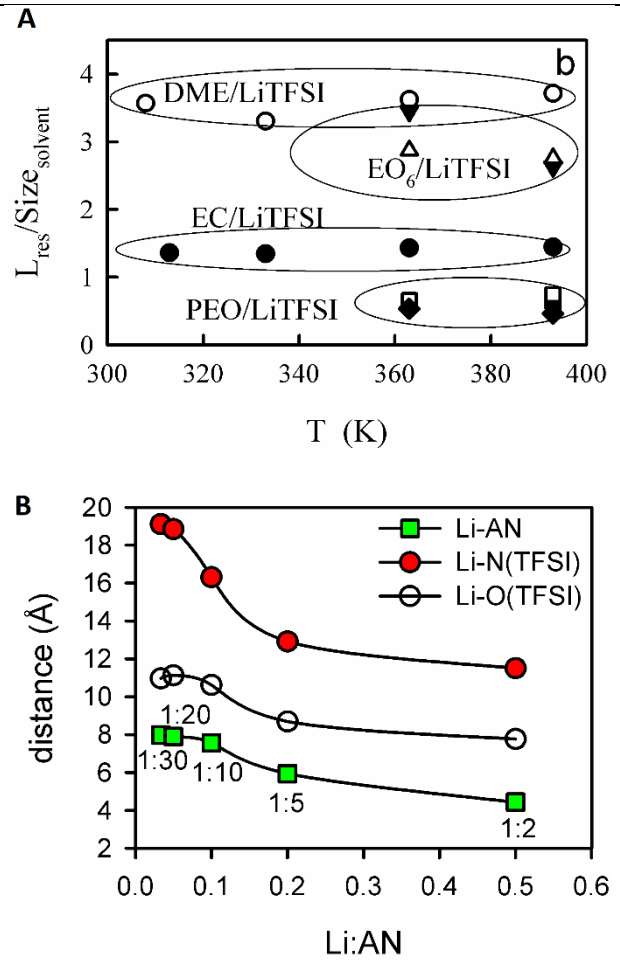
A
b
DME/LiTFSI
EO6/LiTFSI
EC/LiTFSI
PEO/LiTFSI
Lres/Sizesolvent
T (K)
B
Li-AN
Li-N(TFSI)
Li-O(TFSI)
distance (Å)
1:20
1:30
1:10
1:5
1:2
Li:AN

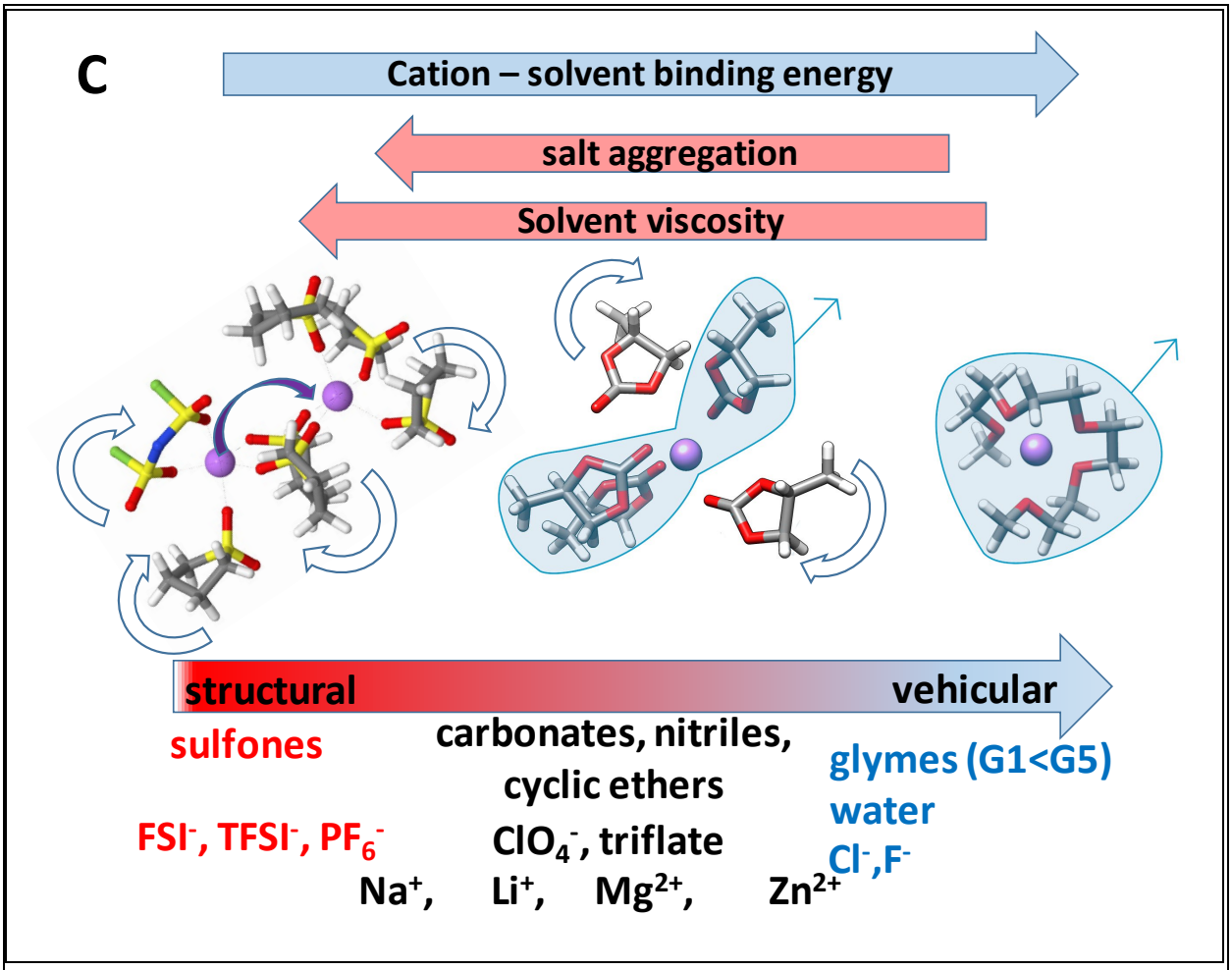

Figure 9: An illustration of the structural (solvent and anion exchange) and vehicular contributions to the cation diffusion. (A) distance a Li^+ diffuses without exchanging solvent (during one Li-solvent residence time) for EC, DME, pentaglyme (G5 or $(EO)_6$) and 54 repeat unit PEO/LiTFSI in the salt-in-solvent regime from MD simulations[58] (Copyright Springer 2007 reproduced with permission); (B) the average distance a Li^+ diffuses without exchanging solvent or TFSI anion nitrogen or oxygen on average using reanalyzed data from Seo et al.[59] as a function of salt concentration; (C) a summary of parameters influencing the structural and vehicular contribution to the metal cation transport in electrolytes.

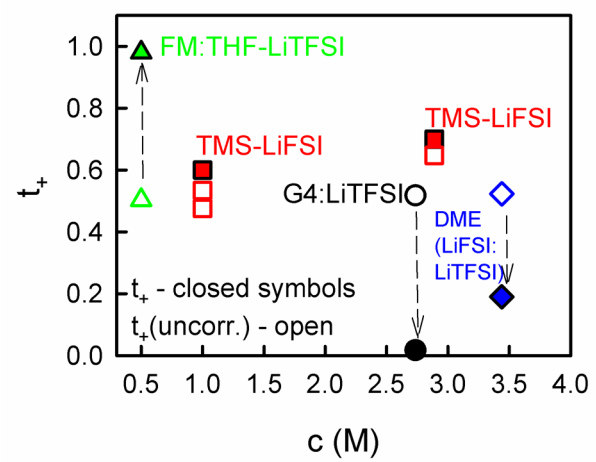

Figure 10. Transferance number calculated assuming uncorrelated (ideal) ion motion ($t_{+\ (ideal)}$) and correlated using formalizm from Wohde et al.[74] for fluoromethane(FM):THF-LiTFSI,[72] post-processing sulfolane (SL)-LiFSI[69], 3.46m LiTFSI+ 3.46m LiFSI in DME,[41] and G4-LiTFSI (Borodin)

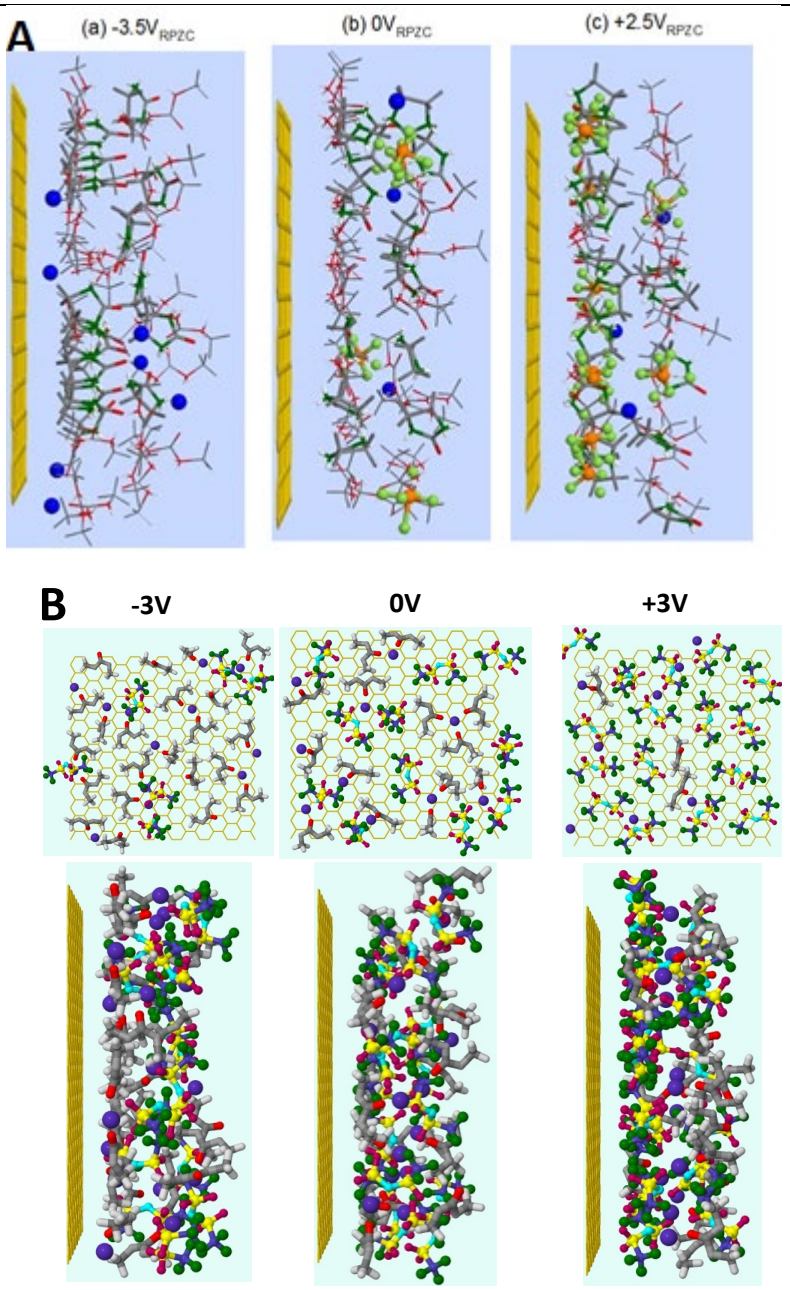

Figure 11. Double layer structure for the salt-in-solvent 1M $LiPF_6$ in EC:DMC(3:7) (A) and solvent-in-salt $DMC_{1.2}TFSI$ electrolytes (B) from MD simulations.[78; 79] Copyright American Chemical Society 2012 and 2017. Reproduced with permission.

References

1. Bard, A.J., and Faulkner, L.R. (2000). Electrochemical Methods: Fundamentals and Applications, 2nd Edition, (New York: John Willey & Sons).
2. Brown, A.P., and Anson, F.C. (1977). Cyclic and differential pulse voltammetric behavior of reactants confined to the electrode surface. Anal. Chem. *49*, 1589-1595.
3. Wang, F., Borodin, O., Ding, M.S., Gobet, M., Vatamanu, J., Fan, X., Gao, T., Edison, N., Liang, Y., Sun, W.*, et al.* (2018). Hybrid Aqueous/Non-aqueous Electrolyte for Safe and High-Energy Li-Ion Batteries. Joule *2*, 927-937.
4. Frumkin, A. (1933). Wasserstoffüberspannung und Struktur der Doppelschicht. Z. Physik. Chem., Ser. A *164*, 121-133.
5. Bockris, J.O.M., Reddy, Amulya K.N. (1998). Modern Electrochemistry https://doi.org/10.1007/b114546 (Kluwer Academic Publishers).
6. Vayenas, C.G., White, Ralph E (1954). Modern Aspects of Electrochemistry, (Butterworth, Washington).
7. Ratner, M.A., and Shriver, D.F. (1988). Ion transport in solvent-free polymers. Chem. Rev. *88*, 109-124.
8. McKinnon, W.R., and Dahn, J.R. (1985). How to Reduce the Cointercalation of Propylene Carbonate in Li x ZrS2 and Other Layered Compounds. J. Electrochem. Soc. *132*, 364-366.
9. Angell, C.A., Liu, C., and Sanchez, E. (1993). Rubbery solid electrolytes with dominant cationic transport and high ambient conductivity. Nature *362*, 137-139.
10. Chen, L., Li, Y., Li, S.-P., Fan, L.-Z., Nan, C.-W., and Goodenough, J.B. (2018). PEO/garnet composite electrolytes for solid-state lithium batteries: From “ceramic-in-polymer” to “polymer-in-ceramic”. Nano Energy *46*, 176-184.
11. Gupta, A., and Sakamoto, J. (2019). Controlling Ionic Transport through the PEO-LiTFSI/LLZTO Interface. Electrochem. Soc. Interface *28*, 63-69.
12. Jeong, S.K., Inaba, M., Iriyama, Y., Abe, T., and Ogumi, Z. (2003). Electrochemical intercalation of lithium ion within graphite from propylene carbonate solutions. Electrochem Solid St *6*, A13-A15.
13. Ueno, K., Yoshida, K., Tsuchiya, M., Tachikawa, N., Dokko, K., and Watanabe, M. (2012). Glyme-Lithium Salt Equimolar Molten Mixtures: Concentrated Solutions or Solvate Ionic Liquids? J. Phys. Chem. B *116*, 11323-11331.
14. Tamura, T., Hachida, T., Yoshida, K., Tachikawa, N., Dokko, K., and Watanabe, M. (2010). New glyme-cyclic imide lithium salt complexes as thermally stable electrolytes for lithium batteries. J. Power Sources *195*, 6095-6100.
15. Tamura, T., Yoshida, K., Hachida, T., Tsuchiya, M., Nakamura, M., Kazue, Y., Tachikawa, N., Dokko, K., and Watanabe, M. (2010). Physicochemical Properties of Glyme-Li Salt Complexes as a New Family of Room-temperature Ionic Liquids. Chem. Lett. *39*, 753-755.
16. Yoshida, K., Nakamura, M., Kazue, Y., Tachikawa, N., Tsuzuki, S., Seki, S., Dokko, K., and Watanabe, M. (2011). Oxidative-Stability Enhancement and Charge Transport Mechanism in Glyme-Lithium Salt Equimolar Complexes. J. Am. Chem. Soc. *133*, 13121-13129.
17. Yoshida, K., Tsuchiya, M., Tachikawa, N., Dokko, K., and Watanabe, M. (2011). Change from Glyme Solutions to Quasi-ionic Liquids for Binary Mixtures Consisting of Lithium Bis(trifluoromethanesulfonyl)amide and Glymes. J. Phys. Chem. C *115*, 18384-18394.
18. Henderson, W.A. (2006). Glyme−Lithium Salt Phase Behavior. J. Phys. Chem. B *110*, 13177-13183.
19. Choquette, Y., Brisard, G., Parent, M., Brouillette, D., Perron, G., Desnoyers, J.E., Armand, M., Gravel, D., and Slougui, N. (1998). Sulfamides and Glymes as Aprotic Solvents for Lithium Batteries. J. Electrochem. Soc. *145*, 3500-3507.

20. Seki, S., Takei, K., Miyashiro, H., and Watanabe, M. (2011). Physicochemical and Electrochemical Properties of Glyme-LiN(SO2F)2 Complex for Safe Lithium-ion Secondary Battery Electrolyte. J. Electrochem. Soc. *158*, A769-A774.
21. Suo, L.M., Hu, Y.S., Li, H., Armand, M., and Chen, L.Q. (2013). A new class of Solvent-in-Salt electrolyte for high-energy rechargeable metallic lithium batteries. Nat. Comm. *4*, 1481.
22. Yamada, Y., Furukawa, K., Sodeyama, K., Kikuchi, K., Yaegashi, M., Tateyama, Y., and Yamada, A. (2014). Unusual Stability of Acetonitrile-Based Superconcentrated Electrolytes for Fast-Charging Lithium-Ion Batteries. J Am Chem Soc *136*, 5039-5046.
23. Wang, J., Yamada, Y., Sodeyama, K., Chiang, C.H., Tateyama, Y., and Yamada, A. (2016). Superconcentrated electrolytes for a high-voltage lithium-ion battery. Nat Commun *7*.
24. Shiga, T., Okuda, C.-a., Kato, Y., and Kondo, H. (2018). Highly Concentrated Electrolytes Containing a Phosphoric Acid Ester Amide with Self-Extinguishing Properties for Use in Lithium Batteries. J. Phys. Chem. C *122*, 9738-9745.
25. Suo, L., Borodin, O., Gao, T., Olguin, M., Ho, J., Fan, X., Luo, C., Wang, C., and Xu, K. (2015). "Water-in-salt" electrolyte enables high-voltage aqueous lithium-ion chemistries. Science *350*, 938-943.
26. Yamada, Y., Usui, K., Sodeyama, K., Ko, S., Tateyama, Y., and Yamada, A. (2016). Hydrate-melt electrolytes for high-energy-density aqueous batteries. Nature Energy *1*, 16129.
27. Suo, L., Borodin, O., Sun, W., Fan, X., Yang, C., Wang, F., Gao, T., Ma, Z., Schroeder, M., von Cresce, A.*, et al.* (2016). Advanced High-Voltage Aqueous Lithium-Ion Battery Enabled by "Water-in-Bisalt" Electrolyte. Angew. Chem. Int. Ed *55*, 7136-7141.
28. Suo, L., Borodin, O., Wang, Y., Rong, X., Sun, W., Fan, X., Xu, S., Schroeder, M.A., Cresce, A.V., Wang, F.*, et al.* (2017). "Water-in-Salt" Electrolyte Makes Aqueous Sodium-Ion Battery Safe, Green, and Long-Lasting. Adv. Energy Mater. 10.1002/aenm.201701189, 1701189.
29. Wang, F., Borodin, O., Gao, T., Fan, X., Sun, W., Han, F., Faraone, A., Dura, J.A., Xu, K., and Wang, C. (2018). Highly reversible zinc metal anode for aqueous batteries. Nat. Mater. *17*, 543-549.
30. Yang, C., Suo, L., Borodin, O., Wang, F., Sun, W., Gao, T., Fan, X., Hou, S., Ma, Z., Amine, K.*, et al.* (2017). Unique aqueous Li-ion/sulfur chemistry with high energy density and reversibility. Proc Natl Acad Sci *114*, 6197-6202.
31. Zhang, C., Holoubek, J., Wu, X., Daniyar, A., Zhu, L., Chen, C., Leonard, D.P., Rodríguez-Pérez, I.A., Jiang, J.-X., Fang, C.*, et al.* (2018). A ZnCl2 water-in-salt electrolyte for a reversible Zn metal anode. Chem. Comm. *54*, 14097-14099.
32. Yang, C., Chen, J., Qing, T., Fan, X., Sun, W., von Cresce, A., Ding, M.S., Borodin, O., Vatamanu, J., Schroeder, M.A.*, et al.* (2017). 4.0 V Aqueous Li-Ion Batteries. Joule *1*, 122-132.
33. Yang, C., Chen, J., Ji, X., Pollard, T.P., Lü, X., Sun, C.-J., Hou, S., Liu, Q., Liu, C., Qing, T.*, et al.* (2019). Aqueous Li-ion battery enabled by halogen conversion–intercalation chemistry in graphite. Nature *569*, 245-250.
34. Xu, K., and Wang, C. (2016). Batteries: Widening voltage windows. Nat. Ener. *1*, 16161.
35. Chen, S., Zheng, J., Mei, D., Han, K.S., Engelhard, M.H., Zhao, W., Xu, W., Liu, J., and Zhang, J.-G. (2018). High-Voltage Lithium-Metal Batteries Enabled by Localized High-Concentration Electrolytes. Adv. Mater. *30*, 1706102.
36. Yu, L., Chen, S., Lee, H., Zhang, L., Engelhard, M.H., Li, Q., Jiao, S., Liu, J., Xu, W., and Zhang, J.-G. (2018). A Localized High-Concentration Electrolyte with Optimized Solvents and Lithium Difluoro(oxalate)borate Additive for Stable Lithium Metal Batteries. ACS Ener. Lett. *3*, 2059-2067.
37. Ren, X., Zou, L., Cao, X., Engelhard, M.H., Liu, W., Burton, S.D., Lee, H., Niu, C., Matthews, B.E., Zhu, Z.*, et al.* (2019). Enabling High-Voltage Lithium-Metal Batteries under Practical Conditions. Joule 10.1016/j.joule.2019.05.006.
38. Chen, S., Zheng, J., Yu, L., Ren, X., Engelhard, M.H., Niu, C., Lee, H., Xu, W., Xiao, J., Liu, J.*, et al.* (2018). High-Efficiency Lithium Metal Batteries with Fire-Retardant Electrolytes. Joule *2*, 1548-1558.

39. Ren, X., Chen, S., Lee, H., Mei, D., Engelhard, M.H., Burton, S.D., Zhao, W., Zheng, J., Li, Q., Ding, M.S*., et al.* (2018). Localized High-Concentration Sulfone Electrolytes for High-Efficiency Lithium-Metal Batteries. Chem *4*, 1877-1892.
40. Huang, Q., Pollard, T.P., Ren, X., Kim, D., Magasinski, A., Borodin, O., and Yushin, G. (2019). Fading Mechanisms and Voltage Hysteresis in FeF_2–NiF_2 Solid Solution Cathodes for Lithium and Lithium-Ion Batteries. Small doi:10.1002/smll.201804670, 1804670-1804610.
41. Alvarado, J., Schroeder, M.A., Pollard, T.P., Wang, X., Lee, J.Z., Zhang, M., Wynn, T., Ding, M., Borodin, O., Meng, Y.S*., et al.* (2019). Bisalt ether electrolytes: a pathway towards lithium metal batteries with Ni-rich cathodes. Ener. Env. Sci. *12*, 780-794.
42. Borodin, O. (2019). Challenges with prediction of battery electrolyte electrochemical stability window and guiding the electrode – electrolyte stabilization. Current Opinion in Electrochemistry *13*, 86-93.
43. Xu, K. (2004). Nonaqueous liquid electrolytes for lithium-based rechargeable batteries. Chem. Rev. *104*, 4303-4417.
44. Bernal, J.D., and Fowler, R.H. (1933). A Theory of Water and Ionic Solution, with Particular Reference to Hydrogen and Hydroxyl Ions. J. Chem. Phys. *1*, 515-548.
45. Seo, D.M., Borodin, O., Han, S.-D., Boyle, P.D., and Henderson, W.A. (2012). Electrolyte Solvation and Ionic Association II. Acetonitrile-Lithium Salt Mixtures: Highly Dissociated Salts. J. Electrochem. Soc *159*, A1489-A1500.
46. Seo, D.M., Borodin, O., Han, S.-D., Ly, Q., Boyle, P.D., and Henderson, W.A. (2012). Electrolyte Solvation and Ionic Association. I. Acetonitrile-Lithium Salt Mixtures: Intermediate and Highly Associated Salts. J. Electrochem. Soc *159*, A553-A565.
47. Han, S.-D., Borodin, O., Seo, D.M., Zhou, Z.-B., and Henderson, W.A. (2014). Electrolyte Solvation and Ionic Association: V. Acetonitrile-Lithium Bis(fluorosulfonyl)imide (LiFSI) Mixtures. J. Electrochem. Soc *161*, A2042-A2053.
48. Wan, C., Hu, M.Y., Borodin, O., Qian, J., Qin, Z., Zhang, J.-G., and Hu, J.Z. (2016). Natural abundance ^{17}O, ^{6}Li NMR and molecular modeling studies of the solvation structures of lithium bis(fluorosulfonyl)imide/1,2-dimethoxyethane liquid electrolytes. J. Power Sources *307*, 231-243.
49. Borodin, O., Suo, L., Gobet, M., Ren, X., Wang, F., Faraone, A., Peng, J., Olguin, M., Schroeder, M., Ding, M.S*., et al.* (2017). Liquid Structure with Nano-Heterogeneity Promotes Cationic Transport in Concentrated Electrolytes. ACS Nano *11*, 10462-10471.
50. Chapman, N., Borodin, O., Yoon, T., Nguyen, C.C., and Lucht, B.L. (2017). Spectroscopic and Density Functional Theory Characterization of Common Lithium Salt Solvates in Carbonate Electrolytes for Lithium Batteries. J. Phys. Chem. C *121*, 2135-2148.
51. Zhang, C., Ueno, K., Yamazaki, A., Yoshida, K., Moon, H., Mandai, T., Umebayashi, Y., Dokko, K., and Watanabe, M. (2014). Chelate Effects in Glyme/Lithium Bis(trifluoromethanesulfonyl)amide Solvate Ionic Liquids. I. Stability of Solvate Cations and Correlation with Electrolyte Properties. J. Phys. Chem. B *118*, 5144-5153.
52. McOwen, D.W., Seo, D.M., Borodin, O., Vatamanu, J., Boyle, P.D., and Henderson, W.A. (2014). Concentrated electrolytes: decrypting electrolyte properties and reassessing Al corrosion mechanisms. Ener.& Env. Sci. *7*, 416-426.
53. Aihara, Y., Sugimoto, K., Price, W.S., and Hayamizu, K. (2000). Ionic conduction and self-diffusion near infinitesimal concentration in lithium salt-organic solvent electrolytes. J. Chem. Phys. *113*, 1981-1991.
54. Borodin, O., Henderson, W.A., Fox, E.T., Berman, M., Gobet, M., and Greenbaum, S. (2013). Influence of Solvent on Ion Aggregation and Transport in PY15TFSI Ionic Liquid–Aprotic Solvent Mixtures. J. Phys. Chem. B *117*, 10581-10588.

55. Aihara, Y., Bando, T., Nakagawa, H., Yoshida, H., Hayamizu, K., Akiba, E., and Price, W.S. (2004). Ion transport properties of six lithium salts dissolved in gamma-butyrolactone studied by self-diffusion and ionic conductivity measurements. J. Electrochem. Soc. *151*, A119-A122.
56. von Wald Cresce, A., Gobet, M., Borodin, O., Peng, J., Russell, S.M., Wikner, E., Fu, A., Hu, L., Lee, H.-S., Zhang, Z*., et al.* (2015). Anion Solvation in Carbonate-Based Electrolytes. J. Phys. Chem. C *119*, 27255-27264.
57. von Wald Cresce, A., Borodin, O., and Xu, K. (2012). Correlating Li^+ Solvation Sheath Structure with Interphasial Chemistry on Graphite. J. Phys. Chem. C *116*, 26111-26117.
58. Borodin, O., and Smith, G.D. (2007). Li^+ transport mechanism in oligo(ethylene oxide)s compared to carbonates. J. Solution. Chem. *36*, 803-813.
59. Seo, D.M., Borodin, O., Balogh, D., O'Connell, M., Ly, Q., Han, S.-D., Passerini, S., and Henderson, W.A. (2013). Electrolyte Solvation and Ionic Association III. Acetonitrile-Lithium Salt Mixtures–Transport Properties. J. Electrochem. Soc *160*, A1061-A1070.
60. Forsyth, M., Yoon, H., Chen, F.F., Zhu, H.J., MacFarlane, D.R., Armand, M., and Howlett, P.C. (2016). Novel Na+ Ion Diffusion Mechanism in Mixed Organic-Inorganic Ionic Liquid Electrolyte Leading to High Na+ Transference Number and Stable, High Rate Electrochemical Cycling of Sodium Cells. J. Phys. Chem. C *120*, 4276-4286.
61. Hayamizu, K., Aihara, Y., Arai, S., and Martinez, C.G. (1999). Pulse-gradient spin-echo H-1, Li-7, and F-19 NMR diffusion and ionic conductivity measurements of 14 organic electrolytes containing LiN(SO2CF3)(2). J. Phys. Chem. B *103*, 519-524.
62. Borodin, O., Giffin, G.A., Moretti, A., Haskins, J.B., Lawson, J.W., Henderson, W.A., and Passerini, S. (2018). Insights into the Structure and Transport of the Lithium, Sodium, Magnesium, and Zinc Bis(trifluoromethansulfonyl)imide Salts in Ionic Liquids. J. Phys. Chem. C *122*, 20108-20121.
63. Dong, D., Sälzer, F., Roling, B., and Bedrov, D. (2018). How efficient is Li+ ion transport in solvate ionic liquids under anion-blocking conditions in a battery? Phys. Chem. Chem. Phys. 10.1039/C8CP06214E.
64. Liyana-Arachchi, T.P., Haskins, J.B., Burke, C.M., Diederichsen, K.M., McCloskey, B.D., and Lawson, J.W. (2018). Polarizable Molecular Dynamics and Experiments of 1,2-Dimethoxyethane Electrolytes with Lithium and Sodium Salts: Structure and Transport Properties. J. Phys. Chem. B *122*, 8548-8559.
65. Dong, D., and Bedrov, D. (2018). Charge Transport in [Li(tetraglyme)][bis(trifluoromethane) sulfonimide] Solvate Ionic Liquids: Insight from Molecular Dynamics Simulations. J. Phys. Chem. B *122*, 9994-10004.
66. Okoshi, M., Chou, C.-P., and Nakai, H. (2018). Theoretical Analysis of Carrier Ion Diffusion in Superconcentrated Electrolyte Solutions for Sodium-Ion Batteries. J. Phys. Chem. B *122*, 2600-2609.
67. Borodin, O., and Smith, G.D. (2009). Quantum Chemistry and Molecular Dynamics Simulation Study of Dimethyl Carbonate: Ethylene Carbonate Electrolytes Doped with LiPF6. J. Phys. Chem. B *113*, 1763-1776.
68. Borodin, O., and Smith, G.D. (2006). LiTFSI Structure and Transport in Ethylene Carbonate from Molecular Dynamics Simulations. J. Phys. Chem. B *110*, 4971-4977.
69. Alvarado, J., Schroeder, M.A., Zhang, M., Borodin, O., Gobrogge, E., Olguin, M., Ding, M.S., Gobet, M., Greenbaum, S., Meng, Y.S*., et al.* (2018). A carbonate-free, sulfone-based electrolyte for high-voltage Li-ion batteries. Materials Today *21*, 341-353.
70. Dokko, K., Watanabe, D., Ugata, Y., Thomas, M.L., Tsuzuki, S., Shinoda, W., Hashimoto, K., Ueno, K., Umebayashi, Y., and Watanabe, M. (2018). Direct Evidence for Li Ion Hopping Conduction in Highly Concentrated Sulfolane-Based Liquid Electrolytes. J. Phys. Chem. B *122*, 10736-10745.
71. Hayamizu, K. (2012). Temperature Dependence of Self-Diffusion Coefficients of Ions and Solvents in Ethylene Carbonate, Propylene Carbonate, and Diethyl Carbonate Single Solutions and

Ethylene Carbonate + Diethyl Carbonate Binary Solutions of LiPF6 Studied by NMR. J. Chem. Eng. Data *57*, 2012-2017.
72. Yang, Y., Davies, D.M., Yin, Y., Borodin, O., Lee, J.Z., Fang, C., Olguin, M., Zhang, Y., Sablina, E.S., Wang, X.*, et al.* (2019). High-Efficiency Lithium-Metal Anode Enabled by Liquefied Gas Electrolytes. Joule 10.1016/j.joule.2019.06.008.
73. Borodin, O., Han, S.-D., Daubert, J.S., Seo, D.M., Yun, S.-H., and Henderson, W.A. (2015). Electrolyte Solvation and Ionic Association: VI. Acetonitrile-Lithium Salt Mixtures: Highly Associated Salts Revisited. J. Electrochem. Soc *162*, A501-A510.
74. Wohde, F., Balabajew, M., and Roling, B. (2016). Li+ Transference Numbers in Liquid Electrolytes Obtained by Very-Low-Frequency Impedance Spectroscopy at Variable Electrode Distances. J. Electrochem. Soc. *163*, A714-A721.
75. Suo, L., Oh, D., Lin, Y., Zhuo, Z., Borodin, O., Gao, T., Wang, F., Kushima, A., Wang, Z., Kim, H.-C.*, et al.* (2017). How Solid-Electrolyte Interphase Forms in Aqueous Electrolytes. J. Am. Chem. Soc. *139*, 18670-18680.
76. McEldrew, M., Goodwin, Z.A.H., Kornyshev, A.A., and Bazant, M.Z. (2018). Theory of the Double Layer in Water-in-Salt Electrolytes. J. Phys. Chem. Lett. *9*, 5840-5846.
77. Vatamanu, J., and Borodin, O. (2017). Ramifications of Water-in-Salt Interfacial Structure at Charged Electrodes for Electrolyte Electrochemical Stability. J. Phys. Chem. Lett. *8*, 4362-4367.
78. Borodin, O., Ren, X., Vatamanu, J., von Wald Cresce, A., Knap, J., and Xu, K. (2017). Modeling Insight into Battery Electrolyte Electrochemical Stability and Interfacial Structure. Acc. Chem. Res. *50*, 2886-2894.
79. Vatamanu, J., Borodin, O., and Smith, G.D. (2012). Molecular Dynamics Simulation Studies of the Structure of a Mixed Carbonate/$LiPF_6$ Electrolyte near Graphite Surface as a Function of Electrode Potential. J. Phys. Chem. C *116*, 1114-1121.
80. Qian, J., Henderson, W.A., Xu, W., Bhattacharya, P., Engelhard, M., Borodin, O., and Zhang, J.-G. (2015). High rate and stable cycling of lithium metal anode. Nat Commun *6*, 6362.
81. Azov, V.A., Egorova, K.S., Seitkalieva, M.M., Kashin, A.S., and Ananikov, V.P. (2018). "Solvent-in-salt" Systems for Design of New Materials in Chemistry, Biology and Energy research. Chem. Soc. Rev. 10.1039/C7CS00547D.
82. Sodeyama, K., Yamada, Y., Aikawa, K., Yamada, A., and Tateyama, Y. (2014). Sacrificial Anion Reduction Mechanism for Electrochemical Stability Improvement in Highly Concentrated Li-Salt Electrolyte. J. Phys. Chem. C *118*, 14091-14097.
83. Yamada, Y., Usui, K., Chiang, C.H., Kikuchi, K., Furukawa, K., and Yamada, A. (2014). General Observation of Lithium Intercalation into Graphite in Ethylene-Carbonate-Free Superconcentrated Electrolytes. ACS Applied Materials & Interfaces *6*, 10892-10899.
84. Cresce, A.v., Russell, S.M., Baker, D.R., Gaskell, K.J., and Xu, K. (2014). In Situ and Quantitative Characterization of Solid Electrolyte Interphases. Nano Lett. *14*, 1405-1412.
85. Dubouis, N., Lemaire, P., Mirvaux, B., Salager, E., Deschamps, M., and Grimaud, A. (2018). The role of the hydrogen evolution reaction in the solid–electrolyte interphase formation mechanism for “Water-in-Salt” electrolytes. Energ. & Env. Sci. *11*, 3491-3499.
86. Lee, M.H., Kim, S.J., Chang, D., Kim, J., Moon, S., Oh, K., Park, K.-Y., Seong, W.M., Park, H., Kwon, G.*, et al.* (2019). Toward a low-cost high-voltage sodium aqueous rechargeable battery. Materials Today https://doi.org/10.1016/j.mattod.2019.02.004.
87. Zheng, J., Tan, G., Shan, P., Liu, T., Hu, J., Feng, Y., Yang, L., Zhang, M., Chen, Z., Lin, Y.*, et al.* (2018). Understanding Thermodynamic and Kinetic Contributions in Expanding the Stability Window of Aqueous Electrolytes. Chem *4*, 2872-2882.

88. Chen, X., Hou, T.-Z., Li, B., Yan, C., Zhu, L., Guan, C., Cheng, X.-B., Peng, H.-J., Huang, J.-Q., and Zhang, Q. Towards Stable Lithium-Sulfur Batteries: Mechanistic Insights into Electrolyte Decomposition on Lithium Metal Anode. Energy Storage Materials http://dx.doi.org/10.1016/j.ensm.2017.01.003.
89. Allen, J.L., Borodin, O., Seo, D.M., and Henderson, W.A. (2014). Combined quantum chemical/Raman spectroscopic analyses of Li+ cation solvation: Cyclic carbonate solvents—Ethylene carbonate and propylene carbonate. J. Power Sources *267*, 821-830.